ADVANCING EARTH AND SPACE SCIENCE

JGR Space Physics

RESEARCH ARTICLE
10.1029/2022JA030919

Key Points:

- The onset of abrupt negative perturbations in H-component at auroral and part of subauroral latitudes coincided with the onset of auroral streamer
- The peak negative bay in H-component at subauroral latitudes coincided with the equatorward extending auroral streamers
- Bright equatorward extended auroral streamers were associated with the peak enhancement in electron flux at geosynchronous orbit

Supporting Information:

Supporting Information may be found in the online version of this article.

Correspondence to:

S. Yadav,
snehay@atmos.ucla.edu

Citation:

Yadav, S., Lyons, L. R., Liu, J., Nishimura, Y., Tian, S., Zou, Y., & Donovan, E. F. (2022). Association of equatorward extending auroral streamers with ground magnetic perturbations and geosynchronous injections. *Journal of Geophysical Research: Space Physics*, *127*, e2022JA030919. https://doi.org/10.1029/2022JA030919

Received 11 AUG 2022
Accepted 23 OCT 2022

Association of Equatorward Extending Auroral Streamers With Ground Magnetic Perturbations and Geosynchronous Injections

Sneha Yadav[1], Larry. R. Lyons[1], Jiang Liu[1,2], Yukitoshi Nishimura[3], Sheng Tian[1], Ying Zou[4], and Eric F. Donovan[5]

[1]Department of Atmospheric and Oceanic Sciences, University of California Los Angeles, Los Angeles, CA, USA, [2]Department of Earth, Planetary, and Space Sciences and Institute of Geophysics and Planetary Physics, University of California Los Angeles, Los Angeles, CA, USA, [3]Department of Electrical and Computer Engineering and Center for Space Physics, Boston University, Boston, MA, USA, [4]Department of Space Science, University of Alabama, Huntsville, AL, USA, [5]Department of Physics and Astronomy, University of Calgary, Calgary, AB, Canada

Abstract Auroral streamers have been found to be a particularly important cause of magnetic perturbations within the auroral oval during substorms. We present a detailed investigation on the association of equatorward extending auroral streamers with ground magnetic perturbations at locations initially equatorward of the auroral oval using Time History of Events and Macroscale Interactions imagers and ground magnetometers. Based on the analysis of four events, we show that negative perturbations in the horizontal (H) component at initially subauroral latitudes were not seen prior to streamer onset, and the peak negative H-bay at subauroral latitudes coincided with the equatorward extending auroral streamers. Although stations close to the poleward boundary of auroral oval showed modest H-component perturbations in response to the substorm onset and poleward auroral intensifications, the abrupt and large responses within the oval were associated with the onset of streamers. Results confirm that ground magnetic perturbations that are traditionally perceived as signatures of magnetic substorm onset are not always an auroral substorm onset but can also be related to auroral streamers. These results are supported by the remarkable correlation of positive bay onset and sudden Pi2 enhancement with the onset of auroral streamers, irrespective of the classical substorm onset. In addition, the magnitude of positive bay and amplitude of Pi2 pulsations, particularly at subauroral latitudes, are enhanced during the events of equatorward extending streamers. In general, all streamer events were accompanied by dipolarization and electron flux enhancement at geosynchronous orbit that continue to strengthen during the emergence of bright streamers.

Plain Language Summary Large, rapid perturbations in the ground magnetic field at high latitudes have been considered a major space weather hazard as they can harm technological systems. Such magnetic perturbations are common at auroral latitudes during geomagnetic storms and substorms. However, it is a matter of research to comprehend under what conditions such perturbations can extend equatorward of the auroral oval. The ground magnetic perturbations at auroral latitudes are shown to be linked with auroral streamers. Auroral streamers are roughly north-south oriented narrow bands of auroral luminosity. They originate near the poleward edge of the auroral oval and propagate equatorward. Auroral streamers are related to flow bursts in the plasma sheet. The equatorward motion of auroral streamer is related to the earthward motion of flow bursts in the plasma sheet. This paper shows that the abrupt magnetic perturbations at latitudes equatorward of the auroral oval (i.e., nominal subauroral latitudes) are linked with the equatorward extending auroral streamers. The observations suggest that as the streamers extended to lower latitudes, the auroral oval expands equatorward to reach previously subauroral latitudes. We found that auroral streamers are, in general, followed by abrupt decreases in the H (horizontal)-component at auroral and subauroral latitudes.

1. Introduction

Large perturbations in the ground magnetic field are a crucial component of space weather. They can be accompanied by rapid perturbations of magnetic field that are directly related to geomagnetically induced currents (GICs), which are known to have a potential impact on high-voltage power transmission networks, oil and gas pipelines, and communication systems (Boteler et al., 1998; Pirjola, 2005). In general, large magnetic perturbations in and near the auroral latitudes have been associated with substorm activities (Akasofu & Aspnes, 1982;

Campbell, 1980). However, many studies showed the association of high latitude magnetic perturbations with more localized magnetospheric/ionospheric processes (Engebretson et al., 2019; Kozyreva et al., 2018; Ngwira et al., 2015, 2018; Pulkkinen et al., 2003; Viljanen, 1997; Weygand et al., 2021).

Auroral streamers have been found to be a particularly important cause of magnetic perturbations in the auroral oval during substorms (Lyons et al., 2013, 2016; Nishimura et al., 2012). They are associated with “meso-scale” ionospheric flow channels (e.g., Gallardo-Lacourt et al., 2014), which are the ionospheric manifestation (Henderson et al., 1998; Kauristie et al., 2003; Nakamura, Baumjohann, Schödel, et al., 2001; Sergeev et al., 2000) of localized fast plasma flows in the plasma sheet, termed bursty bulk flows (BBFs; Angelopoulos et al., 1992, 1994; Baumjohann et al., 1990). Flow channels drive upward field-aligned currents (FAC; Liu, Angelopoulos, Runov, & Zhou, 2013; Liu, Angelopoulos, Zhou, et al., 2013). These FACs lead to the formation of auroral intensifications along the poleward boundary of the auroral oval known as poleward boundary intensifications (PBIs; De la Beaujardière et al., 1994; Lyons et al., 1999; Zesta et al., 2000). As the BBF in the plasma sheet moves earthward, the PBIs extend equatorward from the auroral poleward boundary and align roughly in the north-south (NS) direction becoming auroral streamers.

BBFs in the plasma sheet contain dipolarized magnetic field (Angelopoulos et al., 1994; Liu et al., 2014; Nakamura et al., 2002) and an upward (that forms PBIs and streamers) and downward FAC pair along their edges. This FAC system is the signature of a localized portion of the substorm current wedge (SCW; Birn et al., 1999), also known as a wedgelet (Liu et al., 2015). The SCW is closed by a westward electrojet in the auroral ionosphere (McPherron et al., 1973). The westward electrojet causes a southward perturbation in the ground geomagnetic field in the auroral latitudes (Campbell, 1980; Ngwira et al., 2014; Pulkkinen et al., 2005; Viljanen et al., 2006). This southward perturbation, or a negative perturbation in the H-component (horizontal), is referred to as the negative bay. This current system described above has a sense of nightside “Region 1” (R1) (Iijima & Potemra, 1978). A pair of FACs with the “Region 2” (R2) sense was also found in the dipolarization front/dipolar flux bundle ahead of the R1 FAC (Liu, Angelopoulos, Zhou, et al., 2013). At midlatitude, the two FACs of the SCW create positive perturbations in the H component inside the SCW. The D (eastward) component has an antiasymmetric pattern with a positive maximum near the upward FAC in the premidnight region and a negative minimum in the postmidnight region. This is the classical midlatitude positive bay (MPB) signature (McPherron et al., 1973). The cause of the MPB is a diversion of the tail current through the midnight ionosphere (McPherron, 1972; McPherron et al., 1973). The initiation of a westward electrojet, MPB (e.g., Iijima & Nagata, 1972), and suddenly enhanced Pi2 pulsations (T = 40–150 s; Saito, 1969) observed by ground magnetometers at mid to low latitudes (e.g., Lester et al., 1983; Rostoker, 1968; Sakurai & Saito, 1976) are often considered as signatures of a substorm onset and the initiation of the SCW. However, it is not always true, since Pi2 can also be related to PBIs without substorm onset (Sutcliffe & Lyons, 2002). Large nighttime magnetic perturbation events with hundreds of nT in H can occur well away from substorm onset, and auroral streamers have been identified as one of the key auroral forms that are associated with such magnetic perturbation events (Engebretson et al., 2019; Weygand et al., 2021). Rostoker (1966) and Henderson et al. (2006) also noted that the magnetic bays are not always just positive or negative, but both positive and negative bays can occur at the same station, called as the transition bays.

Auroral streamers occur during both geomagnetic active and quiet conditions, with an increase in number of observations during disturbed conditions (Gabrielse et al., 2018; Paschmann et al., 2012). They are particularly intense and form impulsively and repetitively during the expansion phase of substorms and can exhibit structures such as folds and curls (Hallinan & Davis, 1970; Pritchett et al., 2014). Numerous studies have reported possible signatures of multiple localized currents (wedgelets) that are separated azimuthally by hundreds of km (Forsyth et al., 2014; Kauristie et al., 2000; Liu et al., 2015; Lyons et al., 2012; Palin et al., 2015; Pytte et al., 1976; Rostoker, 1991; Sergeev, 1974). Furthermore, the flow channels associated with auroral streamers have been suggested to be directly related to SCWlet formation (Lyons et al., 2013; Nishimura et al., 2012). Often multiple wedge-type currents are located across the longitude range of the SCW (Nishimura, Lyons, Gabrielse, Weygand, et al., 2020), as has recently been inferred during a storm by Wei et al. (2021).

Henderson et al. (1998) showed that auroral streamers, identified by using satellite UV images, were associated with substorm injections (and/or the arrival of new particle populations) at geosynchronous orbit and were associated with substorm wedgelet-like positive H-bay ground magnetic perturbations on the ground. Sergeev et al. (1999), by using global UV images from the Polar spacecraft, reported the occurrence of auroral streamers in association with the narrow-localized injections (duration about 1–2 min at E = 100 keV and local time extent

≤1 hr MLT) at geosynchronous orbit. However, it is yet to be investigated whether repetitive streamers during a short time interval are associated with repetitive injections at geosynchronous orbit.

Previous studies, as referenced above, highlighted the association of auroral streamers with magnetic perturbations at auroral latitudes. A key factor of GIC excitation is suggested to be the fast medium-scale variations of the geomagnetic field rather than much more intense large-scale current systems (Kozyreva et al., 2018). Given that equatorward propagating auroral streamers represent the flow channel injected energized plasma into the inner magnetosphere, it is important to make a systematic study on the direct association of equatorward moving streamers with rapid magnetic perturbations at high latitudes. Another intriguing question in this context is whether the relationship between auroral streamers and magnetic perturbations can extend equatorward to latitudes that were subauroral at the time of substorm onset. This question has added interest because it may be important for magnetic perturbations and GIC excitation at midlatitudes.

To evaluate the association of equatorward extending streamers with magnetic perturbations equatorward of the auroral oval, we use ground magnetometers and the ground-based ASI (all-sky imager) array (Mende et al., 2008) of the THEMIS (Time History of Events and Macroscale Interactions) mission (Angelopoulos, 2008) to identify auroral streamers. Ground magnetometers distributed from high to low latitudes are used to examine the negative bay onset at auroral and subauroral latitudes and the positive bay and Pi2 pulsations onset at mid and low latitudes in association with evolving streamers. Some of the events we have identified are associated with substorms while others are not. To study the association of auroral streamers with dipolarization and particle flux behavior at the geosynchronous orbit, we used the Geostationary Operational Environmental Satellite (GOES) satellites located over or close to the ASI field-of-view (FOV). We furthermore take advantage of our identification of well-defined streamers and examine the growth time, speed, and lifetime of the auroral streamers, which is still an open question (Forsyth et al., 2020).

2. Data Set and Methodology

The THEMIS ASIs consist of 21 cameras that cover a substantial portion of the auroral oval in North America. Each imager has a latitudinal coverage of ∼9° and longitudinal coverage of ∼2.5 hr magnetic local time (MLT) with time resolution of 3 s and spatial resolution of ∼100 m near zenith (Mende et al., 2008). Auroral streamers were identified as roughly north-south aligned arcs that emerge out from the poleward boundary of the auroral oval or auroral bulge and extend equatorward. Note that auroral streamers can at times be difficult to identify due to other bright aurora in the auroral oval that can be brighter than streamers, and other constraints such as clouds. Therefore, four events presented in this study (Event 1: 16 November 2014 at ∼03:00 to 03:30 UT (∼18:00 to 18:30 MLT), Event 2: 20 March 2013 at ∼05:30 to 06:00 UT (21:00–21:30 MLT), Event 3: 10 February 2013 at ∼07:30 to 08:30 UT (∼20:30 to 21:30 MLT), and Event 4: 02 March 2013 at ∼04:00 to 08:30 UT (20:00–00:30 MLT)) have been chosen based on the clarity of observing the evolution of auroral streamers.

We obtained 1-min ground magnetic field data from the SuperMAG (http://supermag.jhuapl.edu) database (Gjerloev, 2012) to identify the negative bay at auroral and subauroral latitudes associated with auroral streamers. We used the SuperMAG auroral indices SML and SMU (analogous to AL and AU; Newell & Gjerloev, 2011; Gjerloev, 2012) at 1-min cadence.

To closely examine the negative bay onset, positive bay onset, and Pi2 onset in association with auroral streamers, we examined magnetic field variations from auroral to low latitudes using median-subtracted high-resolution magnetometer data (≤1 s). These magnetometers are a part of THEMIS ground-based magnetometer array. We used the ground magnetometers that were located close to the meridian of ASI. To study Pi2 pulsations, the H-component data are processed by band-pass filtering with a passband of 40–150 s.

For the chosen four streamer events, the GOES satellites that were available to study the magnetic field and particle flux behavior at geosynchronous orbit during the streamer activity are GOES-15 (at 135°W GLon) and GOES-13 (at 75°W Glon). The estimated ionospheric footprints of GOES-13 and GOES-15 with respect to the FOV of THEMIS ASIs for the four streamer events are shown in Figure S1 in Supporting Information S1. GOES-15 was located over the FOV of Fort Simpson (FSIM), whereas GOES-13 was over the Gillam ASI FOV. The four streamer events considered in the present study occurred at FSIM, Fort Smith (FSMI), and Fort Yukon (FYKN). GOES-15 was located ∼11°W of the center of FOV of FSIM ASI, whereas ∼30°E of the FYKN ASI. GOES-13 was located 60–90°E with respect to the FOVs of FSIM, FSMI, and FYKN. Magnetic field (MAG) and particle data from MAGnetospheric Electron Detector and MAGnetospheric Proton Detector onboard GOES-15 (Singer et al., 1996) are used to identify the dipolarization and injection signatures at geosynchronous orbit for all four events.

The solar wind parameters (interplanetary magnetic field (IMF)-Bz) and geomagnetic indices (SYM-H/ASY-H) are obtained from the OMNI database. We have used the Space Physics Environment Data Analysis Software tool (Angelopoulos et al., 2019) to download and analyze the geomagnetic activity indices, median subtracted ground-based magnetic field, and GOES data.

3. Observations

We present a detailed investigation on the association of auroral streamers with the H-component magnetic field and dipolarization/particle flux behavior at geosynchronous orbit using four events that occurred on 16 November 2014, 20 March 2013, 10 February 2013, and 2 March 2013. We also studied the evolution of auroral streamers. Here, the time a streamer takes after its onset to achieve its maximum equatorward extent is referred to as the growth time. We estimated the growth time and lifetime of streamers, that is, the time from its onset until they disappear in the ASI FOV. We focus on evolution characteristics of bright, long duration (>30 s) streamers as it is often difficult to monitor rapidly forming weak streamers.

3.1. 16 November 2014, Auroral Streamers Observed at Fort Simpson (Event 1)

Figure 1a shows selected auroral images at FSIM during the period 03:12–03:25 UT of appearance of streamers on 16 November 2014. The whole auroral sequence of auroral activity at FSIM at ∼02:30 to 04:00 UT can be seen in Movie S1 in the auxiliary material. The auroral activity started at ∼02:50 UT with the brightening and poleward movement of the breakup arc, followed by the formation of rapidly evolving active aurora over the FOV of FSIM. The westward surge of aurora over FSIM (see Movie S1) indicates that a substorm-like activity initiated east of FSIM and then the surge propagated to FSIM. Although this intense aurora likely consisted of several embedded auroral structures including streamers, the first clear auroral streamer was seen at ∼03:15 UT. Earlier studies also reported the production of streamers inside the expanding substorm bulges (e.g., Forsyth et al., 2020; Nakamura et al., 1993 for a review). Thereafter, the auroral activity reduced based on decaying auroral emissions. The boundary of the poleward side of the auroral image remained bright and another auroral streamer extended out from the surge poleward boundary at ∼03:19 UT. As this streamer descended equatorward, it exhibited westward motion and considerable structuring particularly at its equatorward edge. The streamer reached around the central latitude of the FOV in ∼1.5 min and had a lifetime of ∼2 min. At 03:21 UT, a striation seems to emerge from the lower latitude and propagate poleward. This striation combined with the detached streamer remnant at ∼03:21:06 UT, forming a bright NS aligned striation. Poleward streamer propagation is rare but has been reported by Liu et al. (2008). Streamer striation has been reported earlier and it is considered as an instability of a flow channel as it propagates earthward (Pritchett et al., 2014). As this NS aligned striation reached near the poleward edge of the FSIM FOV at ∼03:22:15 UT, another streamer extended equatorward at 03:22:30 UT. After its equatorward motion, a bright auroral streamer formed at 03:23–03:24 UT that propagated equatorward and titled westward. This streamer showed considerable structuring known as folds and curls (Hallinan & Davis, 1970). The streamer began to fade as time progressed, but the remnant of the streamer continued around the equatorward boundary until 03:26 UT, giving a lifetime of ∼4.5 min.

Figure 1b shows the variation of IMF-Bz, geomagnetic activity indices (SMU/SML and ASY-H/SYM-H), and H-component magnetic field using 1-min data at auroral and subauroral latitudes on 16 November 2014, at 02:50–03:30 UT. The dashed lines highlight the onset of two streamers. In this and subsequent figures, the magnetic latitude (MLAT) and MLT of different stations at the time of streamer activity are mentioned in the figure. The IMF-Bz remained primarily negative with the peak values of ∼−6 nT at 01–06 UT. The SYM-H index varied between −20 and −40 nT from 01:00 to 03:30 UT. The ASY-H index increased from ∼30 to ∼60 nT (an enhancement of ∼30 nT) from 02:00 to 02:45 UT (i.e., ∼1 hr before the onset of streamers) and streamers started when the ASY-H index reduced to ∼50 nT. The small magnetic field variations at ∼02:00 to 02:30 UT are likely associated with earlier substorm-like activity during this time. The large and abrupt sharp decrease in magnetic field at ∼03:10 to 03:30 UT coincided with the surge and equatorward extending streamers. The maxi-mum decrease is observed at YKC and FSP with the minimum values of ∼−1,000 nT and ∼600 nT, respectively.

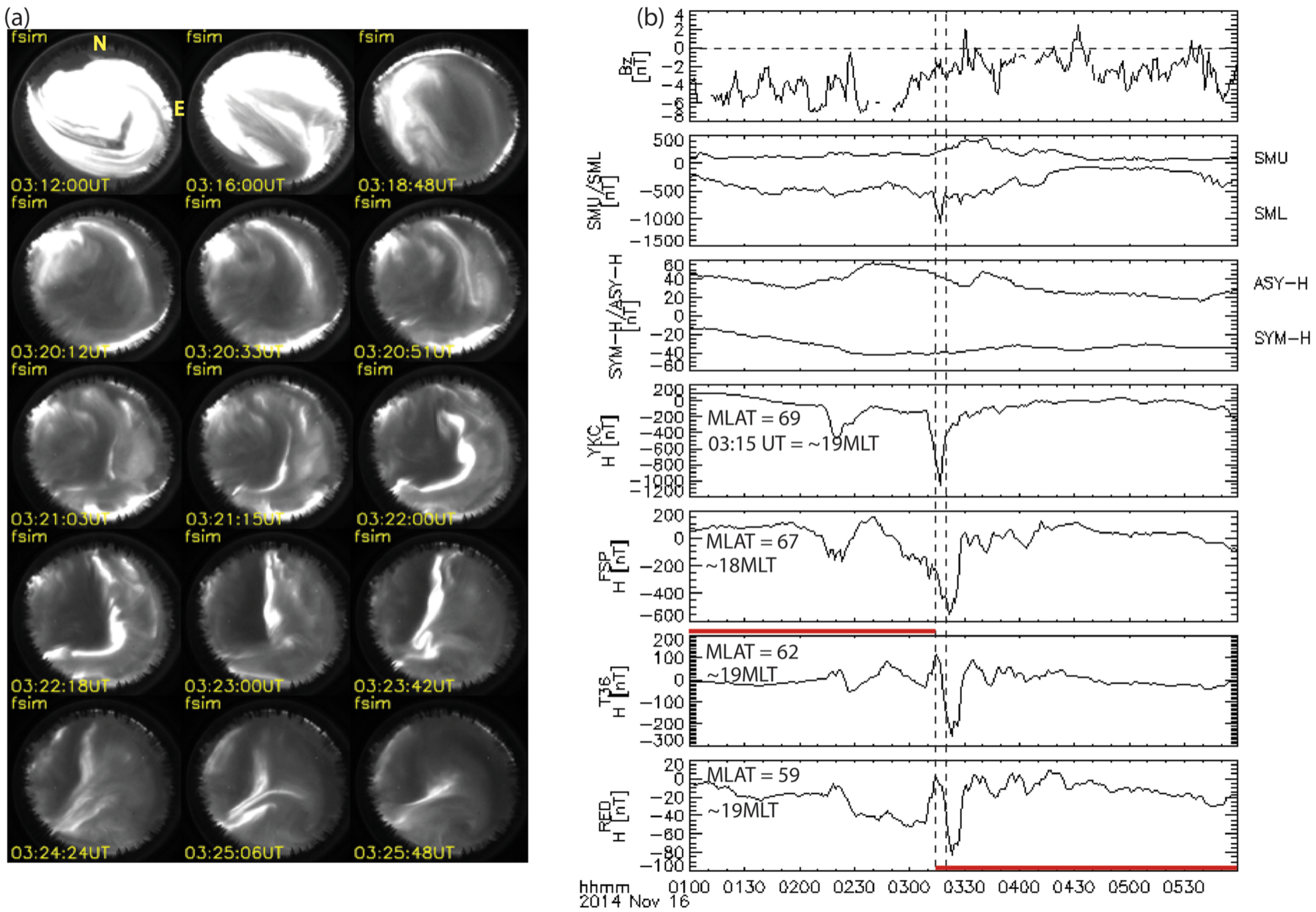

Figure 1. (a) Selected auroral images at Fort Simpson (FSIM) at the time of appearance of auroral streamers on 16 November 2014, at ~03:00 to 03:30 UT. (b) Variation of interplanetary magnetic field-Bz, geomagnetic activity indices (SMU/SML and ASY-H/SYM-H) and H-component magnetic field (at 1-min resolution) at auroral and subauroral latitudes on 16 November 2014, at 01:00–06:00 UT. The dashed lines highlight the onset of auroral streamers.

The magnitude of such a negative bay reduced toward lower latitudes with the minimum values of ~−200 nT at T36 and −80 nT at RED. Coinciding with the surge and streamer activity, the SML index showed a sharp dip of ~500 nT, flanked by dashed lines.

To focus on the sharp decrease in the magnetic field at ~03:20 UT and its association with auroral activity, we present the NS keogram at FSIM and magnetic field data from auroral to low latitudes at 02:50–03:30 UT in Figure 2a. Auroral intensity remained moderate until ~03:10 UT and thereafter rapidly expanded poleward and equatorward. Embedded in the intense aurora, two of the equatorward moving NS structures (streamers) are highlighted by black arrows and their onset is highlighted by black dashed lines. YKC was situated close to the poleward boundary of the auroral oval, whereas FSIM was situated inside the oval. The start of negative bay in the H-component at YKC coincided with the intense poleward expansion of auroral activity. The decrease in the H-component at FSIM also coincided with the time of auroral surge, but the decrease was modest (~−200 nT) and gradual. The start of large negative deflection in H-component at FSIM coincided with onset of the first streamer and the minimum values at ~03:18 to 03:25 UT coincided with the occurrence of the equatorward extended streamers.

The H-component at ATHA and MEA showed positive bay at ~03:12 to 03:18 UT, that is, during the period of expanding aurora suggesting that the contribution of eastward electrojet is larger than the westward electrojet. The defection toward negative values began after ~03:15 UT, that is, after the onset of the first equatorward extending streamer. This kind of sudden excursion in the H-component from positive to negative (or vice versa) is known as the transition bay (Rostoker, 1966). The peak negative H-bay at ATHA and MEA occurred at ~03:23 UT, coincided with the second bright equatorward extending auroral streamer. These observations suggest that as

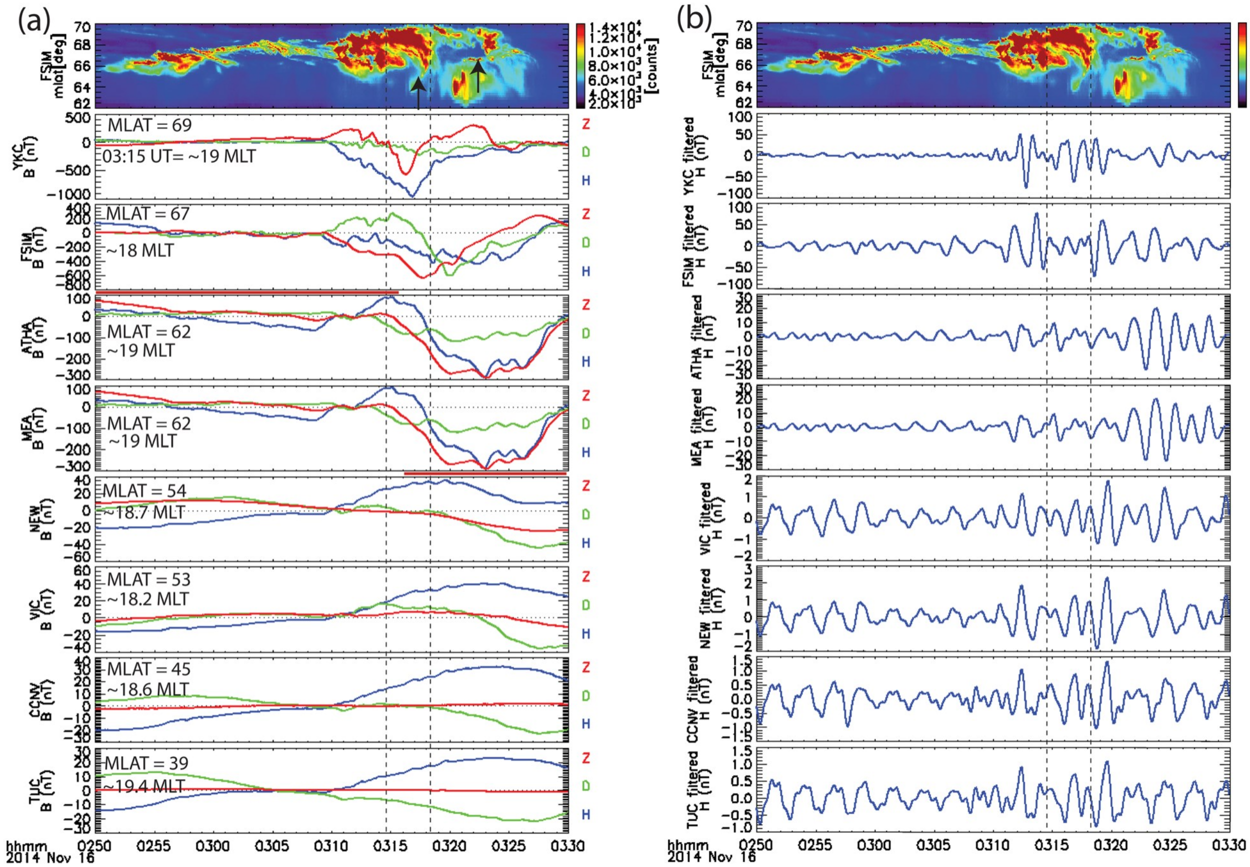

Figure 2. (a) North-south (NS) keogram at Fort Simpson (FSIM; upper panel) and magnetic field data from auroral to low latitudes at 02:50–03:30 UT on 16 November 2014. (b) NS keogram at FSIM (upper panel) and amplitude of Pi2 pulsations in the H-component magnetic field from auroral to low latitudes at 02:50–03:30 UT. Magnetometer data nearly along the same longitude from high to low latitude. The black dashed lines highlight the onset of auroral streamers observed at FSIM.

the streamers extended to lower latitudes, the auroral oval expanded equatorward to reach previously subauroral latitudes (in this case ATHA and MEA), which were slightly below the lower latitude limit of the FSIM ASI FOV. Unfortunately, the ASI data at ATHA was absent for this event; however, the FSIM ASI tells us that the equatorward boundary of the oval was above 62° before ~03:18 UT and then moved equatorward of the FSIM FOV. We thus turned to the ASI data at PINA (50.2°N; 263.9°E), which is situated ~25°E of FSIM ASI, to examine the equatorward expansion of auroral oval after 03:18 UT (see Figure S2 in Supporting Information S1). After 03:10 onward, the auroral oval at PINA expanded equatorward with the boundary of diffuse aurora reaching ~58° MLAT (see Figure S2 in Supporting Information S1). In this and subsequent figures, the horizontal red bar repre-sents the inferred demarcation between auroral and subauroral stations as a function of time, stations above the red bar being within the auroral oval. The H-component at middle latitudes showed increasing trend from ~02:50 UT onward with the appearance of MPB after ~03:10 UT, coinciding with the auroral equatorward expansion that did not expand as far equatorward as the highest latitude (54°) of the midlatitude stations in Figure 2a.

Figure 2b shows the NS keogram at FSIM and the amplitude of Pi2 pulsations in the H-component magnetic field at 02:50–03:30 UT for the stations in Figure 2a. The Pi2 pulsations at lower latitude (VIC, CCNV, NEW, and TUC) stations started concurrently with the intensification of poleward expansion at ~03:10 UT. At YKC and FSIM, the highest amplitude Pi2 pulsations were observed during the poleward and equatorward expanded auroral bulge at ~03:12 to 03:20 UT. However, at subauroral latitudes (ATHA and MEA), the amplitude of the Pi2 pulsations was not the highest around this time. Interestingly, the high amplitude Pi2 pulsations at subauroral latitude during ~03:22 to 03:25 UT coincided with the equatorward extended bright streamers. The onset of Pi2 pulsations at lower latitude stations (VIC, CCNV, NEW, and TUC) coincided with the onset of MPB. At lower

10.1029/2022JA030919

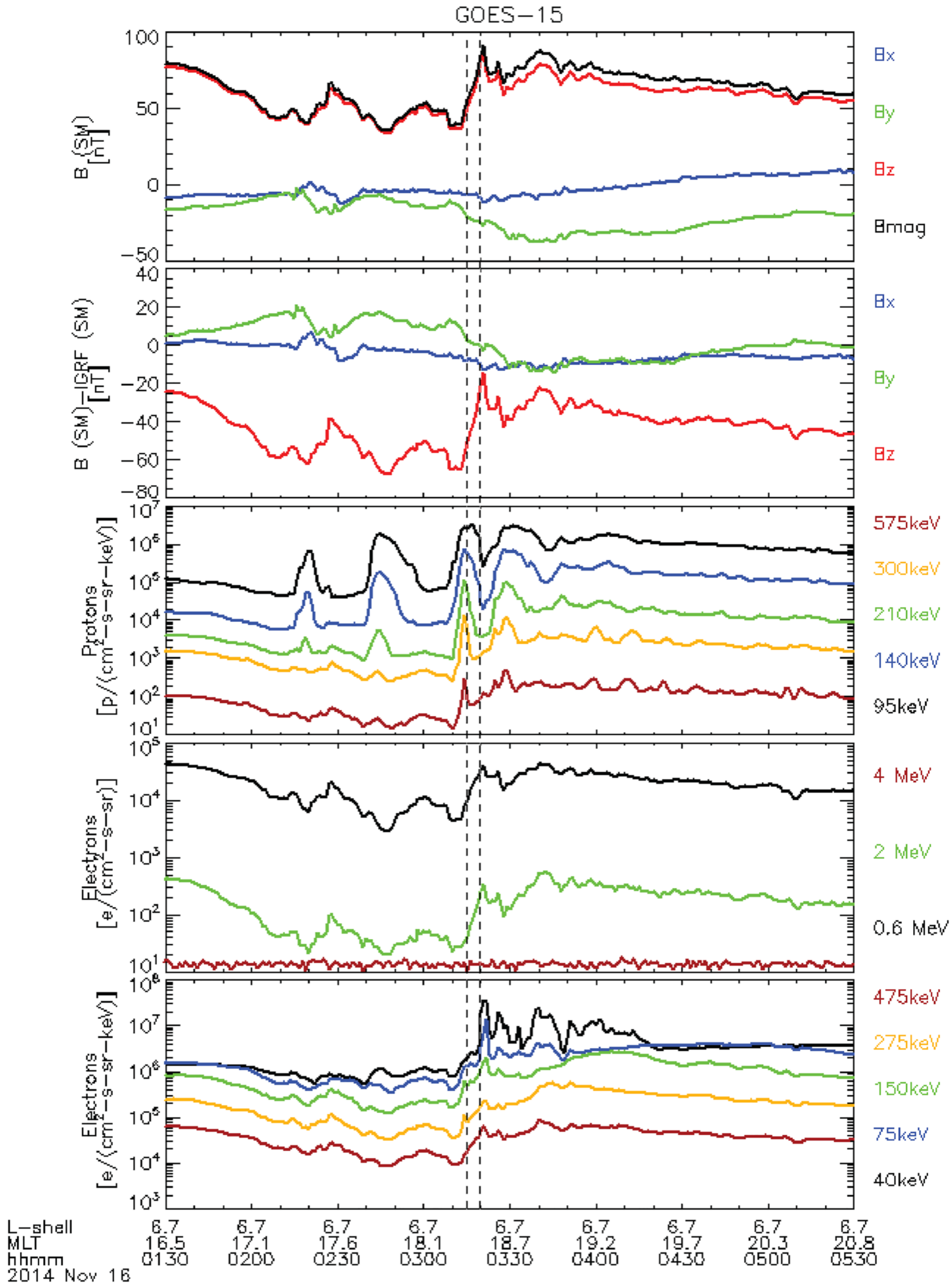

Figure 3. Geostationary Operational Environmental Satellite-15 (GOES-15) observed magnetic field, magnetic field subtracted from the IGRF model, proton flux, and relativistic and nonrelativistic electron flux during ∼01:30 to 05:30 UT as a function of magnetic local time (MLT) and UT on 16 November 2014. The dashed lines highlight the onset time of streamers over FSIM.

latitude stations, the high amplitude Pi2 pulsations were observed at ∼03:10 to 03:13 UT and ∼03:16 to 03:20, coinciding with the onset of expanding auroral bulge and onset of streamer activity, respectively.

In summary, for this event we identified two equatorward extending streamers, both were associated with a negative H-bay that extended to previously subauroral latitudes and Pi2 pulsations at auroral and lower latitudes.

Figure 3 presents the magnetic field, magnetic field subtracted from the IGRF model, proton flux, relativistic and nonrelativistic electron flux during ∼01:30 to 05:30 UT for GOES-15 as a function of MLT and UT. The dashed

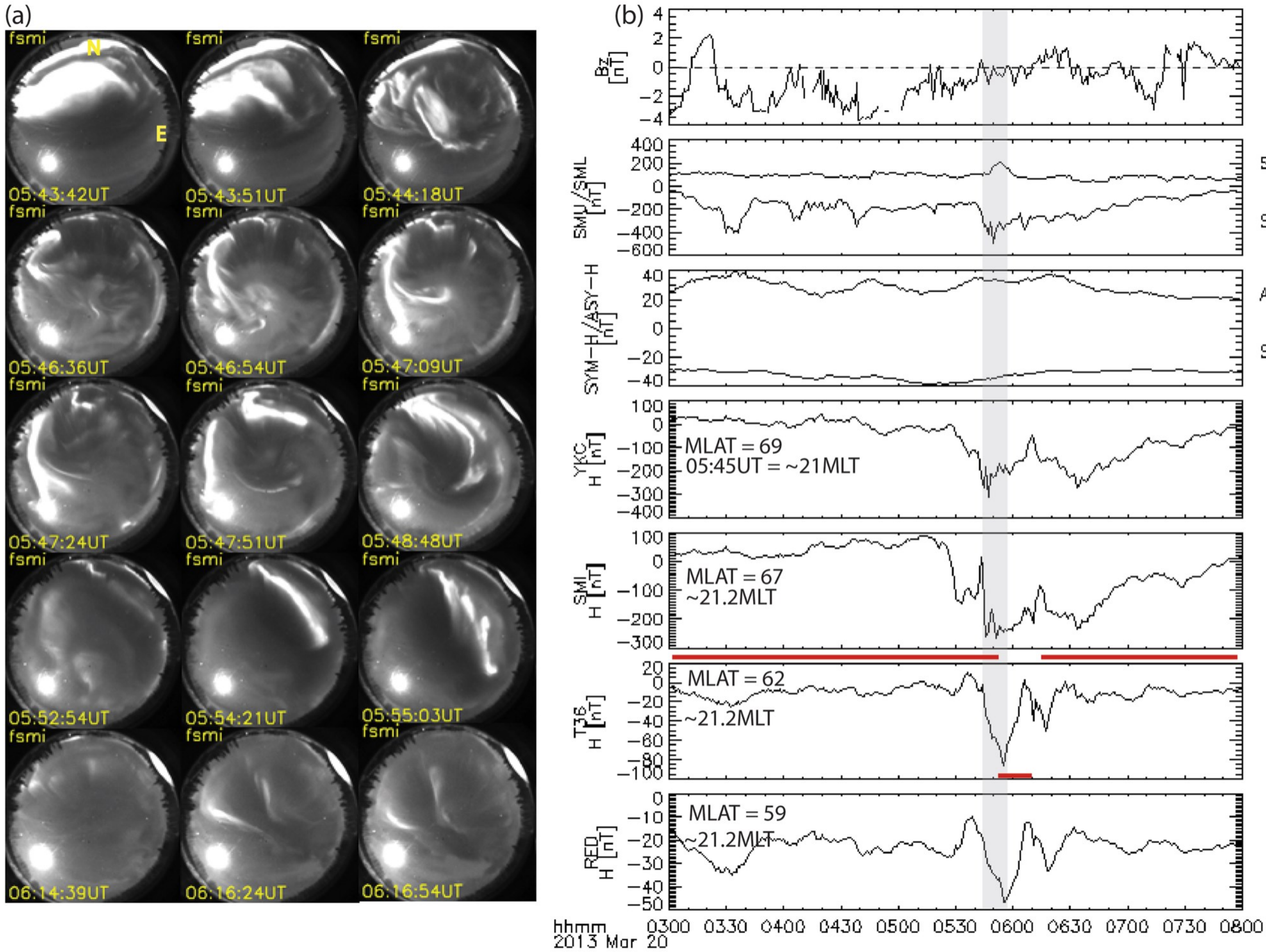

Figure 4. (a) Selected auroral images at Fort Smith (FSMI) at the time of appearance of streamers on 20 March 2013. (b) Variation of interplanetary magnetic field-Bz, geomagnetic activity indices (SMU/SML and ASY-H/SYM-H), and H-component magnetic field (at 1-min resolution) at auroral and subauroral latitudes on 20 March 2013, at 03:00–08:00 UT. The gray bar highlights the onset of streamers. The stations above the horizontal red bar are within the auroral oval.

lines highlight the onset time of streamers over FSIM. GOES-15 was situated in the evening sector (18:00–19:00 MLT) during the streamer activities. GOES-15 observed three dipolarization-like activities. Two small activities began at ~02:20 and ~02:50 UT, and the third dipolarization event began at ~03:12 UT. The electron flux at GOES-15 showed near simultaneous enhancement at all energies except 4 MeV in association with the dipolarization events; however, the increase in protons flux began ~3 to 5 min before the start of dipolarization for all three events. For the first two small dipolarization activities, electron flux increased by a factor of ~2 for the electrons of energies <0.5 MeV and by a factor of 4–5 for the electrons of energies >0.5 MeV. The ASI at FSIM showed substorm-like activity in response to the first dipolarization at GOES-15, not shown. The stream-ers occurred during the third activity, which is sharp in comparison to the previous two activities. The electron flux increased by around an order of magnitude for the third dipolarization activity. Note that the occurrence of bright streamers at ~03:20 to 03:24 UT coincided with the sharp increase in the electron flux, but the electron flux only had a single jump even though multiple streamers occurred. Note that the time resolution of electron flux measurements is 1 min, so it is not possible to resolve the effects of multiple closer jumps corresponding to repetitive streamers.

3.2. 20 March 2013, Auroral Streamers Observed at Fort Smith (Event 2)

For the event occurred on 20 March 2013, five streamer activities were observed within a span of ~10 min at FSMI. Figure 4a shows the auroral images at FSMI at the time of appearance of streamers. The whole auroral sequence of auroral activity at FSMI at 05:00–07:00 can be seen in Movie S2 in the auxiliary material. This event is another substorm event whose auroral onset began at ∼05:27 UT, followed by multiple poleward expansions. From a surge brightening, the first group of auroral streamers emerged at ∼05:43:42 UT. These streamers were transient, disappearing within 30 s of their onset. At 05:46:21 UT, a bright streamer emerged from a poleward arc in the western side of the FOV. This streamer reached near the equatorward edge of the FOV in ∼1 min and disappeared after ∼2 min of its onset. The third streamer began to extend out at ∼05:47:24 UT. It reached near the central latitude of the FOV in ∼1.5 min and disappeared within ∼2 min of its onset. The fourth streamer emerged at ∼05:49:15 UT, became diffuse as it reached near the central latitude of the ASI with a growth time of ∼1 min, and disappeared 2.5 min after of its onset. It is interesting to note the poleward propagating roughly N-S aligned striations emerging from the lower latitudes at 05:49:18–05:50:06 and 05:50:21–05:50:51 UT. At 05:50:54 UT, a bright roughly N-S aligned striation emerged from the lower latitudes, propagated poleward, and covered the central meridian of the ASI within 30 s of its onset. It disappeared at 05:52:48 UT, giving a lifetime of ∼1 min. Thereafter, the fifth streamer slowly emerged out of the PBI at ∼05:52:45 UT, became diffuse and distorted as it reached near the equatorward boundary of the ASI with the growth time of ∼2.5 min, and disappeared in ∼6 min. After the end of the streamer activity, pulsating aurora covered the FOV of FSMI from ∼06:05 onward. Embedded in the pulsating aurora, another set of weak and transient streamers appeared at 06:14-06:18 UT with no clear emergence from the PBI.

Figure 4b shows the variation of IMF-Bz, geomagnetic activity indices (SMU/SML and ASY-H/SYM-H), and H-component magnetic field (at 1-min resolution) at auroral and subauroral latitudes on 20 March 2013, at 03:00–08:00 UT. The vertical gray bar highlights the streamer activities. The IMF-Bz remained primarily negative with the peak values of ∼ −6 nT at ∼03:30 to 05:00 UT (before the onset of streamers) but became close to zero at ∼05:30 to 06:00 (during the period of streamers). The SYM-H index varied between −30 and −45 nT during 03:00–08:00 UT. The ASY-H index showed an enhancement of ∼10 nT at 05:10–05:40 UT, that is just before the onset of streamer activity. In response to the group of streamers at ∼05:43 to 05:58 UT, a large and abrupt decrease in the H-component is observed at all considered stations. The magnitude of such decrease is ∼200 nT at SMI, ∼80 nT at T36, and ∼35 nT at RED. At YKC and SMI, a large negative bay occurred at ∼05:30 to 06:10 UT, corresponding to the period following the substorm onset. However, an abrupt decrease at YKC and SMI at ∼05:43 UT coincided with the surge brightening and onset of streamer activity. The negative bay at T36 and RED started after ∼05:43 UT and peak negative values occurred at ∼05:45 UT, coinciding with the stream-ers, which extended equatorward. The effect of the group of streamers and associated localized sharp dip in the magnetic field is also observed in the global SML index as a sharp decrease of about ∼200 nT. The second event of H-component decrease at ∼06:10 UT might be associated with the second group of weak streamers appearing at ∼06:14 to 06:18 UT over FSMI. To examine the equatorward boundary of auroral oval during streamer activ-ities, we used TPAS ASI (53°N; 259°E; located 11°E of FSMI) because of the absence of images at ATHA. The equatorward boundary of auroral oval at TPAS showed an expansion from ∼05:20 UT, reaching ∼62° MLAT at ∼06:00 UT (see Figure S3 in Supporting Information S1), which is after the appearance of equatorward extended streamers. It is interesting to note that RED also showed considerable negative perturbations in spite of the fact that the equatorward boundary of auroral oval may not have reached to the latitudes of RED.

Figure 5a shows the NS keogram at FSMI (upper panel) and magnetic field variations from auroral to low latitudes at 05:10–06:10 UT on 20 March 2013. Like the first event, in response to the onset of substorm at ∼05:27 UT, the H-component at YKC and FSMI showed a slight decrease, but an abrupt decrease is observed after the surge brightening and onset of streamers at ∼05:43 UT. The subauroral stations (ATHA and MEA) showed a small positive bay at the time of substorm onset at ∼05:30 to 05:43 UT and thereafter started to decrease (transition bay), coinciding with the onset of streamers. The peak negative decrease at subauroral latitudes occurred at ∼05:55 UT, coinciding with the last bright equatorward extending streamer at this time, and thereafter the H-component at subauroral latitudes began to recover. Note that the peak negative H-bay at subauroral latitudes also coincided with the expanded auroral oval that reached near the latitudes of ATHA and MEA (see Figure S3 in Supporting Information S1). The H-component at lower latitudes (PINE, BOU, CCNV, and TUC) showed an increasing trend after the substorm onset until 06:10 UT. The well-defined positive-bay at PINE, BOU, CCNV, and TUC occurred at 05:50–06:10 UT.

Figure 5b shows the NS keogram at FSMI (upper panel) and the amplitude of Pi2 pulsations in H-component magnetic field from auroral to low latitudes at 05:10–06:10 UT for the stations in Figure 5a. The dashed lines highlight the onset of streamers. At YKC (situated equatorward of the poleward boundary of the auroral oval), high amplitude Pi2 pulsations occurred only during the onset of the streamers at 05:43–05:53 UT. At FSMI,

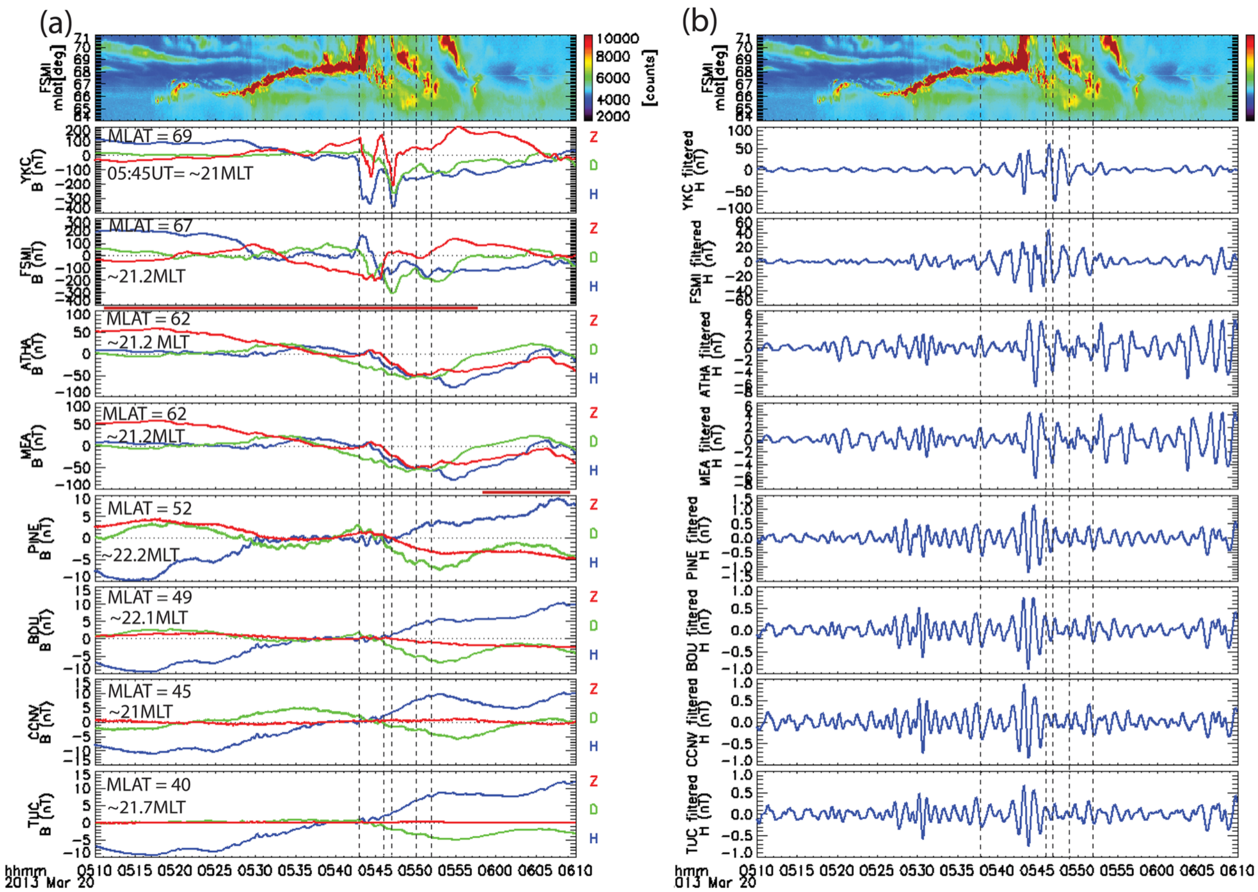

Figure 5. (a) North-south (NS) keogram at Fort Smith (FSMI; upper panel) and magnetic field data from auroral to low latitudes at 05:10–06:10 UT on 20 March 2013. (b) NS keogram at FSIM (upper panel) and amplitude of Pi2 pulsations in the H-component magnetic field from auroral to low latitudes at 05:10–06:10 UT. Magnetometer data nearly along the same longitude from high to low latitude. The black dashed lines highlight the onset of streamers observed at FSMI. The stations above the horizontal red bar are within the auroral oval.

Pi2 pulsations began (at ~05:30 UT) after the substorm onset and intensified during the onset of streamers. At subauroral and middle latitudes, Pi2 pulsations began at 05:20 UT, coinciding with the auroral brightening (see keogram) and showed an intensification during the sudden poleward expansion and onset of streamers. The onset of middle latitude Pi2 pulsations also showed an association with the onset of positive trend in the H-component at these latitudes. The sudden amplification of the Pi2 pulsations at all stations at ~05:43 UT coincided with the onset of streamers. In similarity with Event 1, the amplitude of Pi2 pulsations at ATHA and MEA increased significantly during the appearance of equatorward extended bright streamers at ~05:53 to 05:56 UT, when the equatorward boundary of the auroral oval appeared close to the nominal subauroral latitudes (ATHA and MEA). The amplitude of Pi2 pulsations at ATHA and MEA stations again increased during the appearance of pulsating aurora starting at ~06:02 UT.

In summary, we identified five streamer activities within the span of 10 min. The first event was a weak and transient group of streamers. The subsequent four events were isolated equatorward extended streamers. All the streamers were followed by a negative H-bay at previously subauroral latitudes and associated with Pi2 pulsations at auroral and lower latitudes.

Figure 6 presents the magnetic field, magnetic field subtracted from the IGRF model, proton flux, and relativistic and nonrelativistic electron flux for GOES-15 as a function of MLT and UT on 20 March 2013, at ~03:00 to 08:30 UT. GOES-15 was in the premidnight sector (20:00–21:30 MLT) when the streamers were observed over FSMI, highlighted by a gray shaded bar. Note that GOES-15 is located ~11°W of FSMI. GOES-15 observed a sharp decrease in Bz followed by an abrupt increase at ~05:26 UT, coinciding with the substorm onset at FSMI. Embedded in the continuously increasing trend at ~05:26 to 07:00 UT, Bmag and Bz showed high-frequency

10.1029/2022JA030919

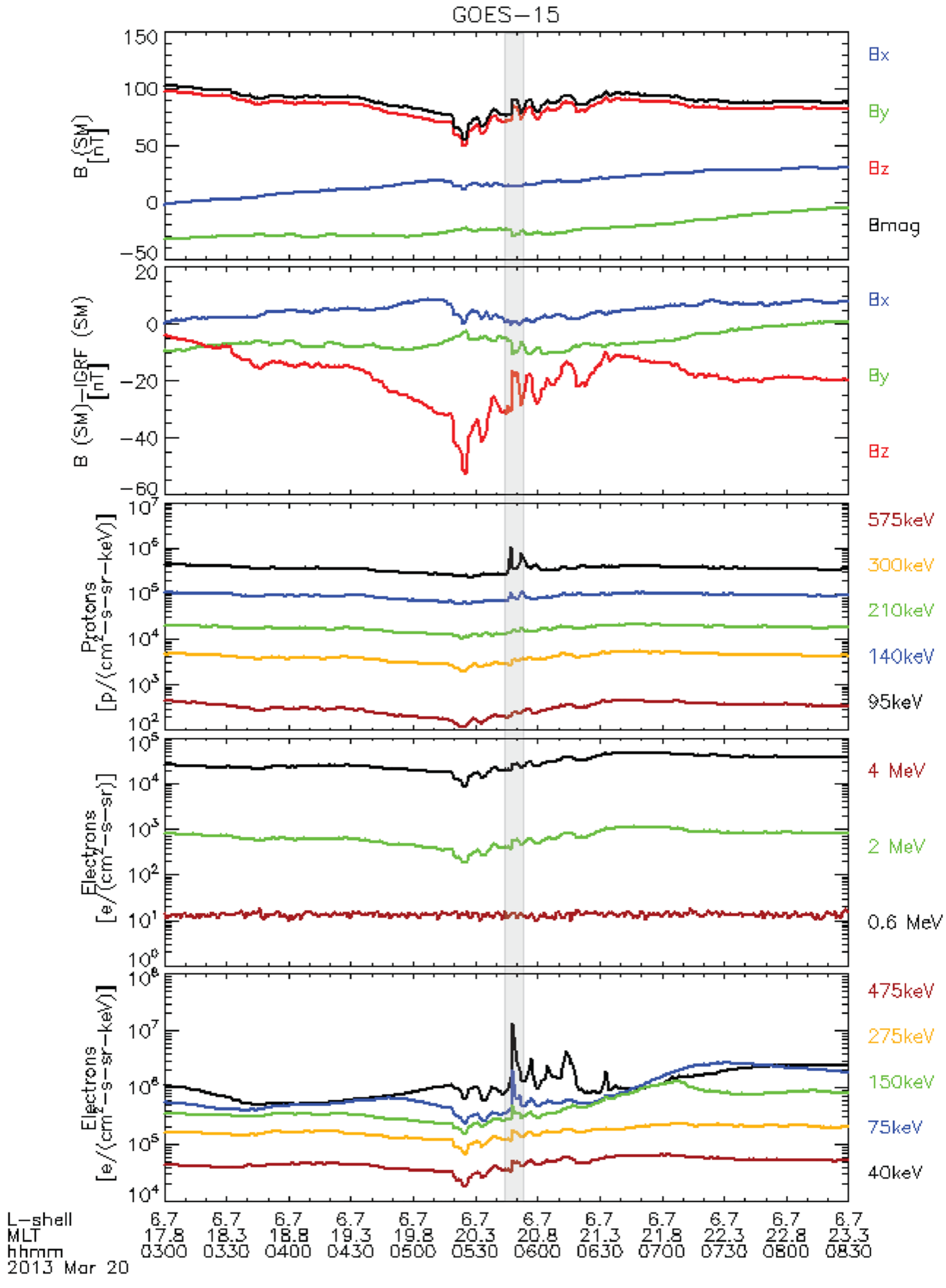

Figure 6. Geostationary Operational Environmental Satellite-15 (GOES-15) observed magnetic field, magnetic field subtracted from the interplanetary magnetic field model, proton flux, and relativistic and nonrelativistic electron flux during ∼03:00 to 08:30 UT as a function of magnetic local time (MLT) and UT on 20 March 2013. The dashed lines highlight the onset time of streamers over Fort Smith.

variations. In association with the dipolarization at ∼05:26 UT, the electron flux at all energies except 4 MeV showed a simultaneous increase. Unlike the electron flux, the proton flux showed slight perturbations but no considerable enhancement in response to the dipolarization at ∼05:26 UT. In similarity with Bmag and B, the electron flux at all energies (except 4 MeV) showed small-scale high-frequency perturbations. The perturbation at ∼05:45 UT is interesting as all five streamers occurred around this abrupt increase. At 05:43–05:48 UT, the electron flux at lower energies (40 and 75 keV) showed an enhancement by around an order of magnitude, whereas the electron flux at higher energies (150 keV–2 MeV) showed an enhancement by a factor of ∼2. The

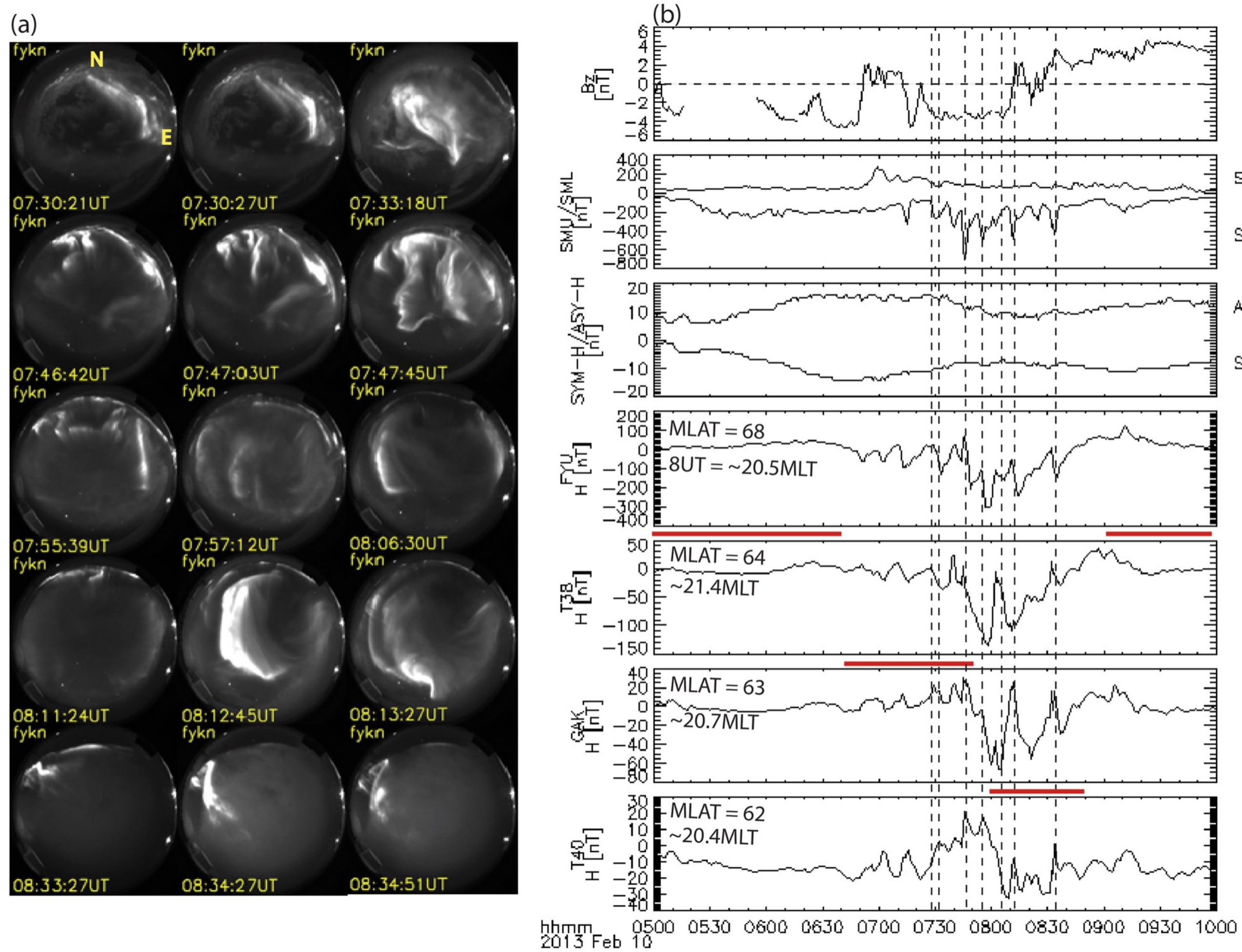

Figure 7. (a) Selected auroral images at Fort Yukon (FYKN) at the time of appearance of streamers on 10 February 2013. (b) Variation of interplanetary magnetic field-Bz, geomagnetic activity indices (SMU/SML and ASY-H/SYM-H), and H-component magnetic field (at 1-min resolution) at auroral and subauroral latitudes on 10 February 2013, at 05:00–10:00 UT. The dashed lines highlight the onset of streamers. The stations above the horizontal red bar are within the auroral oval.

proton flux at 95–140 keV energy channels also showed an enhancement by a factor of ~2 to 5 at ~05:45 UT. Note that all five streamer activities coincided with this sharp increase in the particle flux (both electron and proton).

3.3. 10 February 2013, Auroral Streamers Observed at Fort Yukon (Event 3)

For the event of 10 February 2013, several streamer activities (both isolated and group of streamers) occurred within the span of ~1 hr at FYKN. Figure 7a shows the auroral images at FYKN at the time of appearance of streamers on 10 February 2013. The whole auroral sequence of auroral activity at FYKN at 07:00–08:40 UT can be seen in Movie S3 in the auxiliary material. At ~07:00 to 07:30 UT, the FOV of FYKN was filled with clouds, making it difficult to associate bright auroral streamers with auroral onset or PBI. Despite the clouds, the first set of auroral streamers emerging from the eastern edge of the auroral oval appeared at ~07:29 UT. While slowly moving westward, the streamer reached near the central pixel of the ASI in ~1.5 min and disappeared after 2.5 min of its onset. With the disappearance of this streamer, a group of streamers, consisting of continuously emerging streamers, appeared at ~07:31:18 to 07:33:30 UT. The lifetime of this streamer group was ~4 min as the remnants of this streamer group appeared until ~07:34 UT before it merged with the background aurora. At ~07:39 to 07:44 UT, the weak emission structures were observed in the eastern side of auroral oval. Third streamer activity which began at ~07:46:21 UT consisted of a group of multiple streamers. At ~07:47 UT, a group of streamers extended equatorward and reached near the central pixel of the ASI in ~1 min. The eastward side streamer detached itself from the poleward boundary, leaving a bright blob of aurora at ~07:48 to 07:48:12 UT. From this bright blob, a poleward propagating roughly NS oriented striation emerged at ~07:48:21 UT. It reached near the central pixel of the ASI FOV within 30 s, became diffuse, moved equatorward, and disappeared at ~07:49:30 UT. Because of the continuous activity from the poleward boundary of the auroral oval and lower latitude, bright streamers occurred at ~07:48 to 07:49 UT. The remnants of these streamers appeared until 07:52 UT, implying that the lifetime of the streamer group was ~6 min. At 07:55–07:57:30 UT, several weak, diffuse streamers emerged near the poleward boundary and disappeared within 15–30 s of their formation. For the fifth streamer activity, an auroral streamer gradually began to emerge out at ~08:05 UT in the western side of the FOV. It reached near the equatorward edge of the ASI in ~2.5 min. This isolated streamer slowly propagated westward, became diffuse, and disappeared after ~4 min of its onset. There might be a possibility that it moved out of the FOV of the imager. The sixth streamer activity began when an isolated streamer emerged out at ~08:11:30 UT. As this streamer extended equatorward, it brightened and showed splitting at ~08:12:48 UT. The streamer slightly tilted eastward at its equatorward end, making a C-shape structure. As it further moved equatorward, the poleward side of the streamer became diffuse while the equatorward edge remained brightened. This isolated streamer reached close to the equatorward boundary after ~2 min of its onset. This streamer detached from the poleward boundary, whereas the equatorward side of the streamer remained bright. Interestingly, after the detachment from the poleward boundary, the remnant streamer at the equatorward side began moving poleward, reached near the central pixel, became diffuse, and disappeared at ~08:15 UT. The seventh eastward titled streamer began to emerge out at ~08:32 UT from the PBI and extended equatorward. Because of the presence of clouds in the FOV, the equatorward extent of the streamer cannot be clearly identified. The lifetime of this streamer was ~2 min.

Figure 7b shows the variation of IMF-Bz, geomagnetic activity indices (SMU/SML and ASY-H/SYM-H), and H-component magnetic field using 1-min data at auroral and subauroral latitudes on 10 February 2013, at 05:00–10:00 UT. The dashed lines correspond to the onset times of the streamer activities in the ASI. The IMF-Bz remained primarily negative at ~05:00 to 06:30 UT. It attained northward orientation for ~30 min before it again turned in the southward direction at ~07:15 UT with the peak values of ~ −4 nT. The SYM-H index varied between 0 and −15 nT during 05:00–07:30 UT. The ASY-H index showed an enhancement of ~10 nT at 05:00–06:00 UT and maintained high values until 07:40 UT. The streamer activity coincided with the sharp negative bay in the H-component at auroral and subauroral latitudes. In general, all streamer activities were followed by a sharp decrease in the H-component. The maximum decrease occurred at ~07:55 to 08:10 UT. The maximum decrease was ~300 nT at FYU, ~130 nT at T38, −60 nT at GAK, and −30 nT at T40. The effect of these streamers is also observed in the global SML index in terms of abrupt negative deflection of ~200 to 400 nT coinciding with streamers.

Figure 8a shows NS keogram at FYKN (upper panel) and magnetic field variations from auroral to low latitudes at 07:20–08:50 UT on 10 February 2013. We plotted the magnetograms from auroral to low latitude available close to the meridian of FYKN. In the keogram, streamers appeared in terms of patches of intense emission moving equatorward. The onset time of streamers is highlighted by black dashed lines. At FYKN (located closest to the auroral poleward boundary), the onset of negative bay in H-component coincided with the intensification in the poleward boundary and onset of streamers. Being located inside the auroral oval, CMO showed small negative perturbations with respect to the PBIs and streamers at ~07:30 to 07:50 UT. To examine the location of subauroral latitude with respect to auroral oval, we used GAKO ASI (62.4°N, 214.8°E) (see Figure S4 in Supporting Information S1). The auroral oval at GAKO showed an equatorward expansion from ~07:50 UT onward and the equatorward boundary of auroral oval appeared close to ~62° MLAT at ~08:10 to ~08:50 UT, coinciding with the appearance of equatorward extended streamers. GAKO (an initial subauroral station) acquired positive values at ~07:30 to 07:50 UT. The onset of negative deflection at GAKO occurred after ~07:47 UT, coinciding with the bright equatorward extending streamers, indicated by black arrow. The abrupt decrease in the H-component at FYKN and CMO also coincided with this equatorward extending streamer. The peak negative bay at FYKN, CMO, and GAKO coincided with the streamers that reached close to the equatorward boundary, indicated by black arrows. Note the sharp recovery of H-component at CMO and GAKO at 08:00–08:05 UT in the absence of streamer activity at this time. The H-component at MCGR showed positive values at ~07:30 to 08:00 UT and thereafter started to decrease. The decrease at MCGR was also considerably lower as compared to that observed at GAKO. This might be associated with the fact that GAKO was inside the auroral oval whereas MCGR was situated near the equatorward boundary of the auroral oval. The mid- and low-latitude stations did not show coherent positive-bay structure as observed in the previous two cases. SIT and VIC showed decreased values and did not

10.1029/2022JA030919

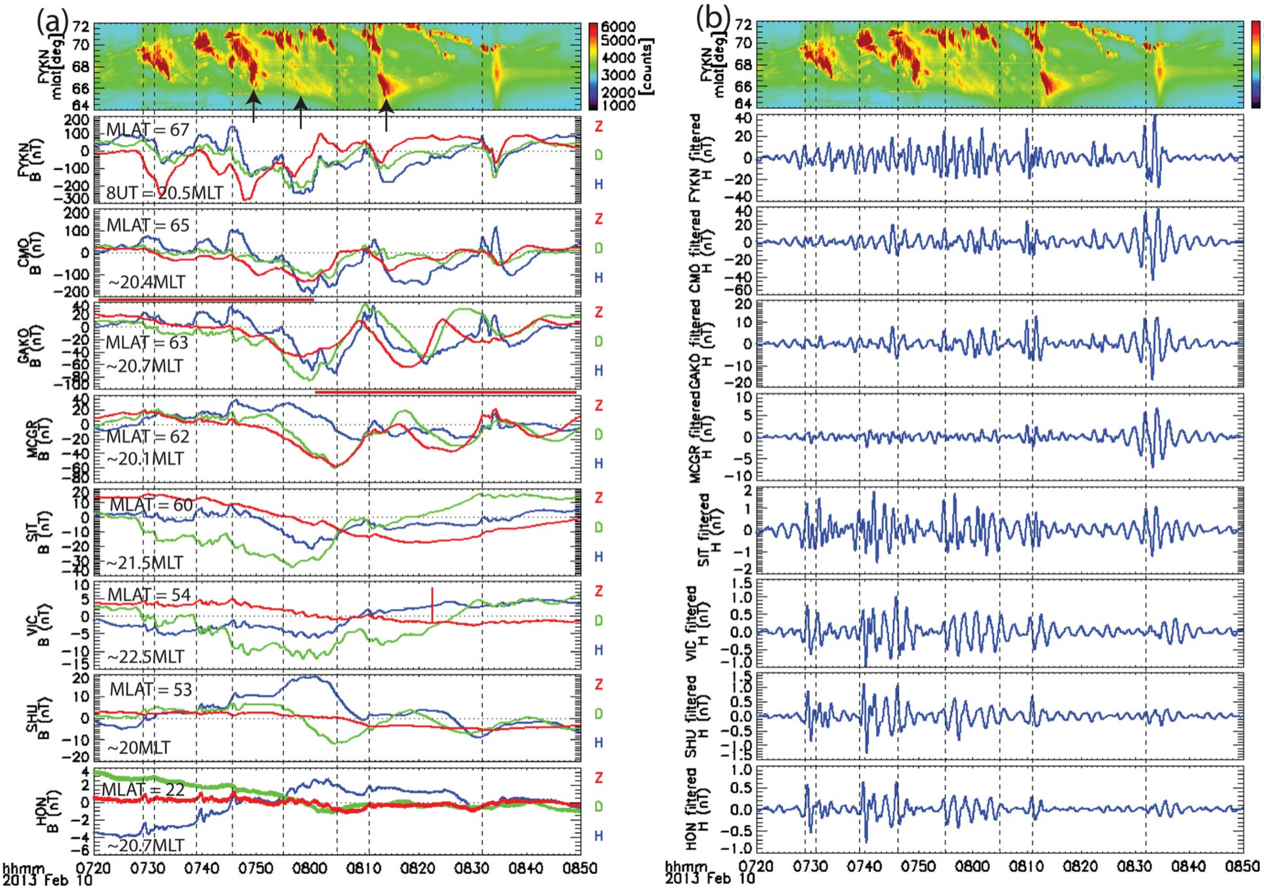

Figure 8. (a) North-south (NS) keogram at Fort Yukon (FYKN; upper panel) and magnetic field variations from auroral to low-latitudes at 07:20–08:50 UT on 10 February 2013. (b) NS keogram at FYKN and amplitude of Pi2 pulsations in the H-component magnetic field from auroral to low latitudes at 07:20–08:50 UT. Magnetometer data nearly along the same longitude from high to low latitude. The black dashed lines highlight the onset of streamers observed at FYKN. The stations above the horizontal red bar are within the auroral oval.

show MPB structure. However, SHU and HON showed H-component positive bay at ∼07:45 to 08:30 UT when bright equatorward streamers were observed. It is also interesting that with each of the streamers, except for the fifth and sixth, which were distinctly separated in time, an abrupt positive perturbation was observed at the two lowest latitude stations.

Figure 8b shows the NS keogram at FYKN and amplitude of Pi2 pulsations in the H-component magnetic field from auroral to low latitudes at 07:20–08:50 UT for the stations in Figure 8a. The onset of every PBI or poleward auroral intensification coincided with the onset of a new set of high amplitude Pi2 pulsations at mid and low latitudes. At mid and low latitudes, the decrease in the amplitude of Pi2 pulsations between the two PBIs can be noted. Unlike the previous two events, continuous Pi2 pulsations occurred at FYKN (located close to the poleward boundary of the auroral oval) with an intensification during the appearance of bright streamers. The Pi2 pulsation activity at CMO and GAKO remained very small except for the events when the equatorward extended streamers occurred, that is, at 07:46, 08:00, 08:10, and 08:33 UT. At MCGR, Pi2 pulsation activity occurred at ∼08:10 and 08:33 UT, coinciding with the bright, equatorward extended streamers. The magnitude of the Pi2 pulsations at MCGR was also smaller than that observed at GAKO, coinciding with GAKO being inside the auroral oval whereas MCGR was near the equatorward boundary of the auroral oval.

In summary, for this event within the span of ∼1 hr, 8 streamer activities occurred. The first two streamer activities consisted of a weak and transient group of streamers. The following three streamer events consisted of an equatorward extending and repetitive group of streamers. The subsequent three streamers were isolated equatorward extending streamers. The H-component at subauroral latitudes began to decrease after the appearance of the third streamer activity, which consisted of equatorward extended streamers. The negative H-bay at subauroral

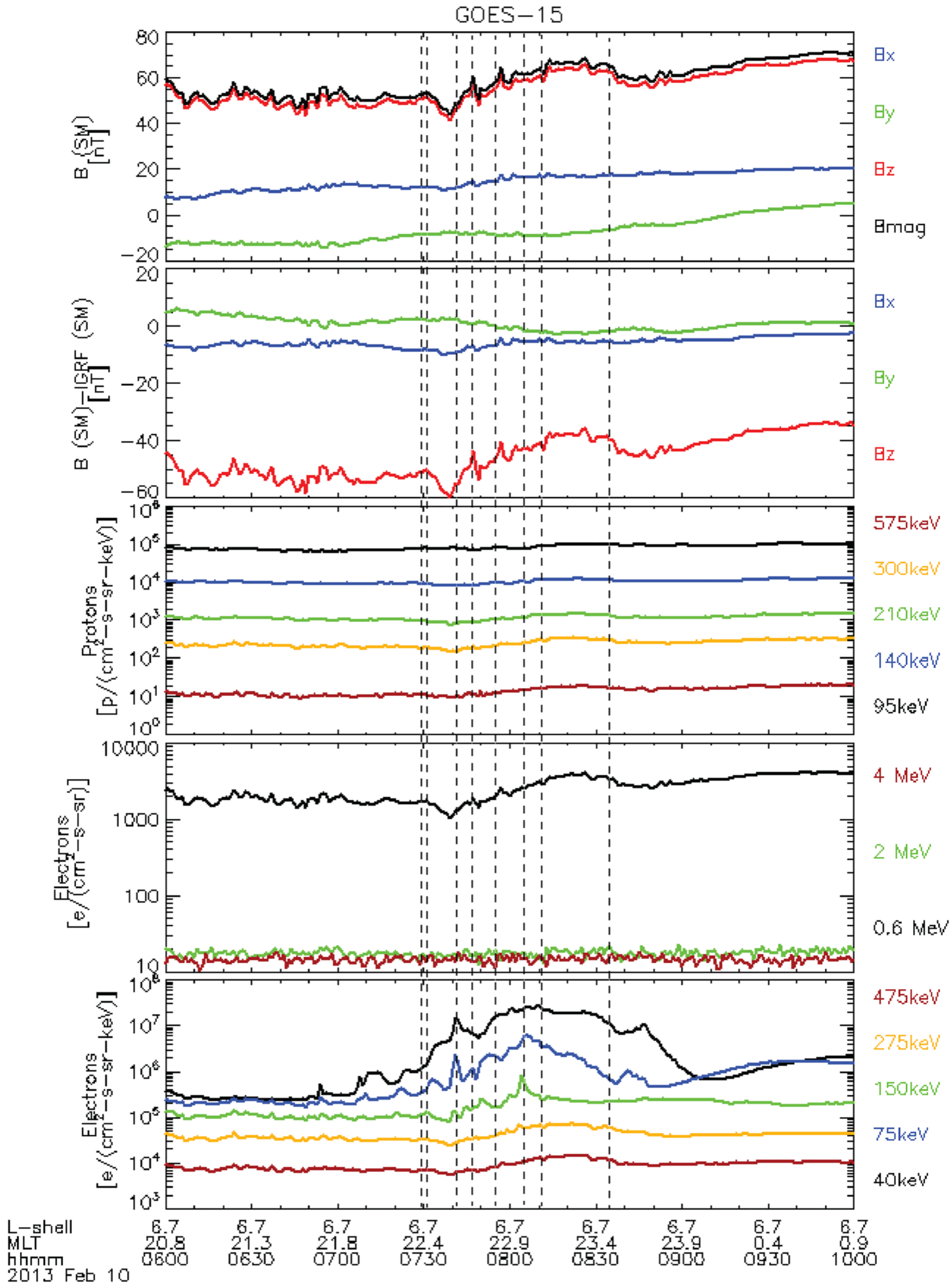

Figure 9. Geostationary Operational Environmental Satellite-15 (GOES-15) observed magnetic field, magnetic field subtracted from the interplanetary magnetic field model, proton flux, and relativistic and nonrelativistic electron flux during ~06:00 to 10:00 UT as a function of magnetic local time (MLT) and UT on 10 February 2013. The dashed lines highlight the onset time of streamers over Fort Yukon.

latitudes coincided with the occurrence of equatorward extended streamers. All streamer activities including the PBI events were associated with the Pi2 pulsations at auroral and lower latitudes.

Figure 9 presents the magnetic field, magnetic field subtracted from the IGRF model, proton flux, and relativistic and nonrelativistic electron flux during ~06:00 to 10:00 UT for GOES-15 as a function of MLT and UT on 10 February 2013. The dashed lines highlight the onset of streamers. Although GOES-15 is located ~30°E of FYKN ASI, it could still provide some insights on the dipolarization activity and particle flux behavior at

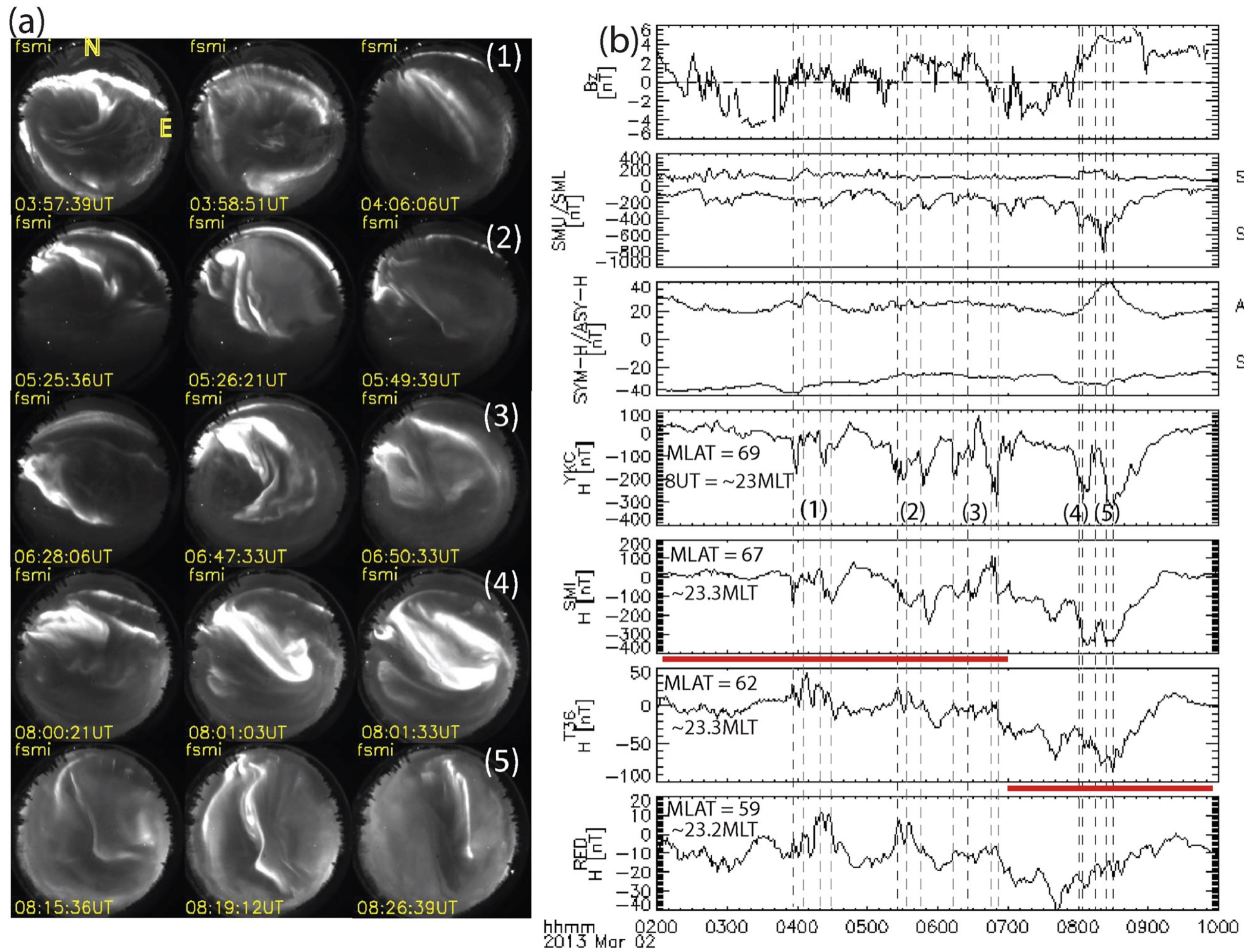

Figure 10. (a) Selected auroral images at Fort Smith (FSMI) at the time of appearance of streamers on 2 March 2013. (b) Variation of interplanetary magnetic field-Bz, geomagnetic activity indices (SMU/SML and ASY-H/SYM-H), and H-component magnetic field (at 1-min resolution) at auroral and subauroral latitudes on 2 March 2013, at 02:00–10:00 UT. The dashed lines highlight the onset of streamers. The stations above the horizontal red bar are within the auroral oval.

geosynchronous orbit during the streamer activity. GOES-15 was in the premidnight sector (22:30–23:30 MLT) during the streamer activities. GOES-15 observed a small enhancement in Bz (dipolarization) at ~07:40 UT and after that Bz continued to increase gradually until 08:25 UT with embedded small-scale perturbations. The electron flux at lower energies (40–75 keV) began to show gradual increase after 07:00 UT, well before the dipolarization activity. The electron flux at higher energies (150 keV–0.6 MeV) showed enhancement after 04:40 UT that coincided with the dipolarization. This indicates that GOES-15 observed a dispersed increase in the electron flux and the injection region might be located west of GOES-15. The proton fluxes showed no considerable change in association with this dipolarization activity or before that, as expected from the spacecraft being to the east of the streamers. The electron flux at lower energies (40–150 keV) showed fluctuations, not observed at higher energies (275 keV–4 MeV). In general, all the streamers occurred during the enhancement in electron flux, and the bright equatorward streamer at ~08:10 UT coincided with the peak in the electron flux at 40–150 keV. These observations suggest the association of auroral streamers with dipolarization and injection activity at geosynchronous orbit.

3.4. 2 March 2013, Auroral Streamers Observed at Fort Smith (Event 4)

For the event of 2 March 2013, several streamer activities (both isolated and streamer group) occurred at four different time intervals within the span of 5 hr. These different time intervals of streamer activity are marked from (1) to (5) in Figure 10a, which shows the auroral images at FSMI at the time of appearance of streamers.

The whole auroral sequence of auroral activity at FYKN at 03:40–09:00 UT can be seen in Movie S4 in the auxiliary material. The first streamer activity began at ∼03:57:30 UT that is during the expansion phase of a substorm. During the expansion phase, several short duration (∼5 to 10 s), diffuse streamers emerged from the surge poleward boundary until ∼04:01 UT. Another three sets of weak, diffuse streamers occurred at ∼04:05 to 04:08, 04:20 to 04:24, and 04:29 to 04:31 UT.

The second set of streamers began with the intensification of the poleward boundary of the auroral oval. An auroral streamer began to extend out at ∼05:25:24 UT. This streamer titled eastward as it extended equatorward, and a roughly NS feature began to emerge at its eastward side at ∼05:26:15 UT and extended equatorward until 05:26:45 UT, leading to the formation of two NS aligned striation. These two NS aligned striation merged at 05:27 UT, forming a bright NS aligned striation at 05:27–05:27:30 UT and disappeared at ∼05:28 UT. Thereafter, several weak, diffuse, and repetitive activity occurred on several occasions between ∼05:30 and 06:30 UT. For instance, at 05:33:45 to 05:37:40, ∼05:47:30 to 05:52:00, and ∼06:14:12 to 06:16:06 UT.

The third activity started with the emergence of an eastward titled streamer at ∼06:27 UT from the westward boundary of the auroral oval activity. This streamer aligned in the east-west direction and gradually shifted toward the south-east direction. This streamer was followed by an auroral bulge after 1.5 min of its onset. After a period of ∼10 min of inactivity, the poleward boundary again intensified at ∼06:40 to 06:45 UT. Thereafter, repetitive streamers emerged out from the PBI at ∼06:46:50 to 06:51:30 UT.

The fourth set of streamers began at 08:00:21 UT when an eastward tilted streamer emerged from the poleward auroral bulge. As it moved equatorward, it developed significant structuring and split into two streamers. It reached the central pixel of the FOV after ∼1 min of its onset and followed by the formation of an auroral bulge, which covered nearly the entire FOV of the ASI. In the background of diffuse emissions, another bright eastward titled streamer emerged out at ∼08:02:15 UT. It reached near the equatorward boundary after ∼1 min of its onset and became indistinguishable after ∼2.5 min of its onset.

For the fifth set of streamers at ∼08:14 to 08:30 UT, several groups of streamers emerged from different meridi-ans of the FOV. This activity started with the appearance of a weak, diffuse streamer at 08:14 UT. As this diffuse streamer propagated equatorward, another streamer emerged from the western side of the FOV at ∼08:15 UT and extended equatorward. The diffused streamer reached around the central pixel of the FOV in about 1.75 min. It is interesting to note the continuous equatorward and poleward flow type activity along the diffused streamer at 08:16:15–08:18:30 UT (see Movie S4 in the auxiliary material). From the PBI, the apparent equatorward flow type activity at 08:18:15–08:20:18 UT led to the formation of very bright equatorward extended multiple streamers at ∼08:18:30 to 08:21:30 UT. These different sets of streamers showed ribbon-like motion along the streamer and continued to exist until 08:23 UT because of the continuously flow type activity from the poleward boundary, implying a lifetime of ∼9 min. An isolated streamer emerged at ∼08:25:15 UT. It reached around the central latitude of the FOV after ∼1.25 min of its onset. As time progressed, this streamer brightened again at ∼08:29:30 because of the emergence of another streamer and disappeared after ∼6 min of its onset.

Figure 10b shows the variation of IMF-Bz, geomagnetic activity indices (SMU/SML and ASY-H/SYM-H), and H-component magnetic field using 1-min data at auroral and subauroral latitudes on 2 March 2013, at 02:00–10:00 UT. The dashed lines correspond to the onset time of the streamer activity. The stations above the horizontal red bar are the auroral latitudes. The IMF-Bz was mainly southward at 03:00–04:00 and 07:00–08:00 UT, with the peak negative values of ∼−4 nT. At 04:00–07:00, the IMF-Bz was mainly northward with occasional southward deflection. The ASY-H index showed an increase of ∼13 nT from 03:00 to 04:00 UT, that is, before the onset of first streamer activity. Before the onset of second and third streamer activity, the ASY-H index exhibited an increase of ∼8 nT. The ASY-H index again began to increase from ∼07:40 UT and showed a significant enhancement of ∼25 nT at ∼08:40 UT. Note that the southward IMF-Bz and significant enhancement in ASY-H index at 08:00 UT were associated with the intense equatorward extending streamers. The SYM-H index during 02:00–10:00 UT was around ∼−30 to −40 nT, indicating moderate geomagnetic activity. In general, the decrease in H-component at auroral and subauroral stations was preceded by auroral surge and streamer activities. We used the ATHA ASI to estimate the equatorward boundary of the auroral oval (see Figure S5 in Supporting Informa-tion S1). Despite the clouds, the equatorward expansion of the oval was observed during the auroral surge and streamer activities. T36 appears to be slightly outside or close to the equatorward boundary of the auroral oval, whereas RED was situated equatorward of the auroral oval at ∼04:15 to 06:50 UT. In response to the continuous streamer activities after ∼08:00 onward, the auroral oval expanded and the FOV of ATHA ASI seems to be filled

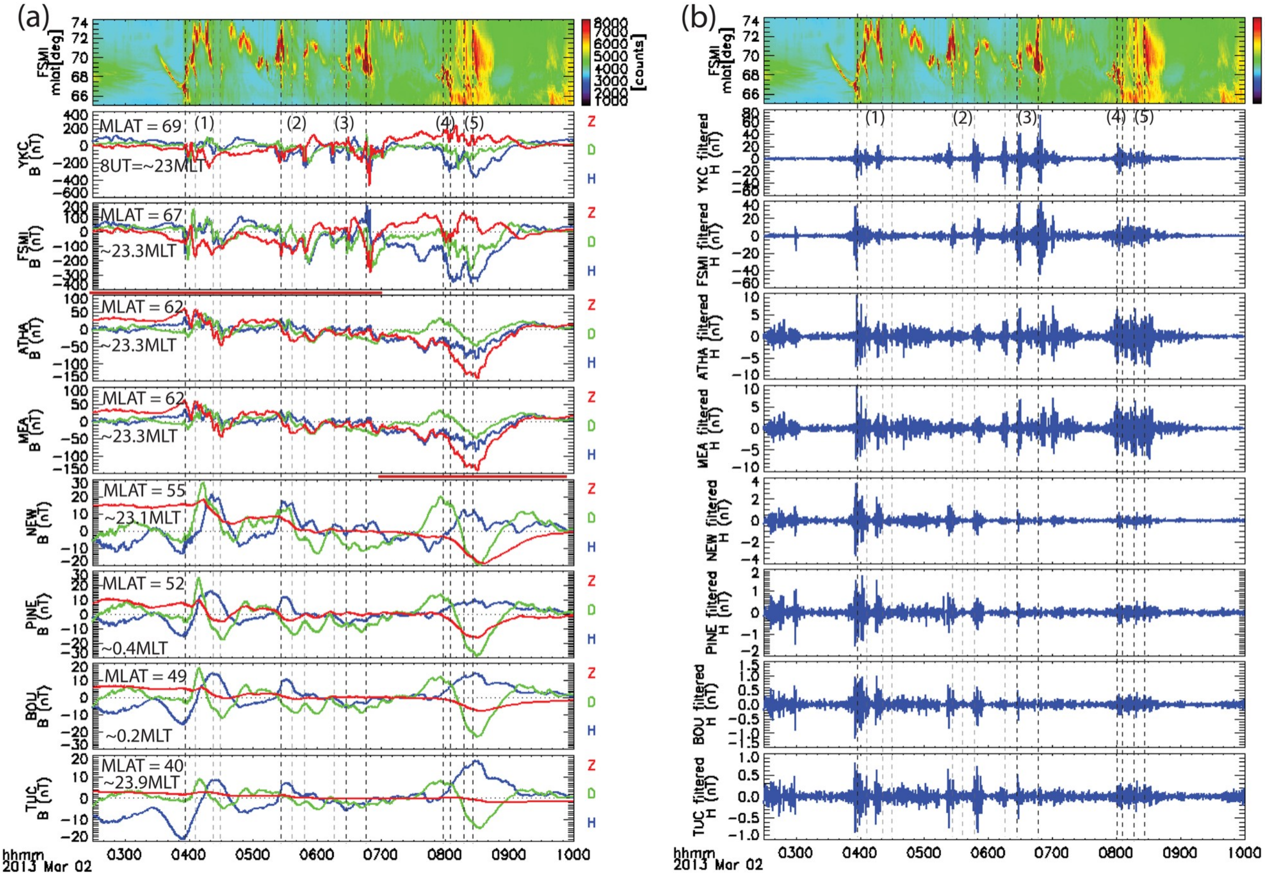

Figure 11. (a) North-south (NS) keogram at Fort Smith (FSMI; upper panel) and magnetic field variations from auroral to low latitudes at 02:30–10:00 UT on 2 March 2013. (b) NS keogram at FSMI (upper panel) and amplitude of Pi2 pulsations in the H-component magnetic field from auroral to low latitudes at 02:30–10:00 UT on 2 March 2013. Magnetometer data nearly along the same longitude from high to low latitude. The black dashed lines highlight the onset of streamers observed at FSMI. The stations above the horizontal red bar are within the auroral oval.

with the pulsating diffuse emissions. Both T36 and RED (initial subauroral latitudes) were inside the diffuse emission boundary of the auroral oval after ∼07:00 onward. Although RED did not show one-to-one correlation, the effect of streamer activity and equatorward expanding auroral oval is apparent in terms of abrupt perturbations and continuous decrease in the magnetic field. Continuous presence of streamers during ∼03:55 to 08:30 UT leads to the decreasing trend in the H-component at all stations. The H-component decreased by ∼300 nT at YKC and SMI, ∼80 nT at T36, and ∼40 nT at RED. The effect of continuous streamer activity is also observed in the global SML index in terms of small negative deflections. The intense equatorward extending auroral stream-ers at ∼08:15 to 08:30 UT coincided with the large decrease of ∼ −400 nT in the SML index.

Figure 11a shows auroral keogram at FSMI (upper panel) and magnetic field variations from auroral to low latitudes at 02:30–10:00 UT on 2 March 2013. The black and gray dashed lines highlight the onset of bright and weak streamers, respectively. The five-streamer activities are marked from (1) to (5) in the keogram. After the growth phase of ∼25 min, a substorm onset occurred at ∼03:55 UT and several short duration streamers began to emerge at ∼03:57 to 04:30 UT. The negative deflection at YKC and FSMI began immediately after the substorm onset. ATHA and MEA (situated near the equatorward boundary of the auroral oval at ∼03:50 to 04:10 UT) showed a slight decrease of ∼5 nT after the onset of streamer activity at ∼03:57 UT. The middle latitude stations showed increasing trend starting at 03:55 UT and a positive bay at ∼04:05 to 04:40 UT. The classical substorm auroral onset features (equatorward moving growth phase arc followed by a rapid poleward movement) as observed for event (1) are not observed for the subsequent four streamer events. In general, for all the streamer activity events, the decrease in H-component at YKC, which is situated inside the auroral oval, coincided with the auroral intensification. The decrease in H-component at FSMI, ATHA, and MEA began after 07:00 UT, coinciding with the equatorward expansion of the auroral oval due to continuous equatorward extended streamer activity. In response to the bright equatorward extending streamers at 08:00–08:30 UT (Events 4 and 5), the H-component at YKC, FSMI, ATHA, and MEA showed a significant negative bay. A significant positive bay is observed at middle latitude stations for bright equatorward extending streamer activity events (Events 4 and 5). Note that for events (4) and (5) the amplitude of the positive bay at middle latitude were comparable to that observed for event (1) which was associated with classical auroral onset at FSMI. The positive bay at middle latitudes is also observed for event (2) but not discernible for streamer event (3).

Figure 11b shows the NS keogram at FSMI (upper panel) and the amplitude of Pi2 pulsations in H-component magnetic field from auroral to low latitudes at 02:30–10:00 UT for the stations in Figure 11a. The onset of substorm for event (1) was associated with significant Pi2 pulsation activity at auroral and lower latitudes. The amplitude of Pi2 pulsations increased with the onset of streamers at high latitudes at ~03:57 UT. In general, the onset of high amplitude Pi2 pulsations at lower latitudes were associated with the onset of PBI/auroral intensification and streamers for all five events. The high latitude stations showed the onset of high amplitude pulsations with the onset of streamers. For event (3), the high amplitude Pi2 pulsations were observed prominently for auroral and subauroral latitudes when equatorward extending streamers were observed. At subauroral latitudes, the highest amplitude Pi2 pulsations were observed for events (4) and (5) when bright equatorward extending streamers occurred. The lower latitude stations also demonstrated moderate Pi2 pulsation activity for these two bright equatorward extending streamer events (4 and 5), whereas the Pi2 pulsations were very low for event (3) at middle latitudes.

In summary, for the event of 2 March 2013, several streamer activities occurred within the span of 5 hr. We identified seven isolated equatorward extending streamers. Five isolated equatorward extending streamers occurred during Events 4 and 5. In general, the streamer activities for Events 1, 2, and 3 were followed by small negative H perturbations at subauroral latitudes, but the large negative H bay occurred during Events 4 and 5 when intense equatorward extending streamers occurred. All the streamer activities were associated with Pi2 pulsations at auroral and lower latitudes.

Figure 12 presents the magnetic field, magnetic field subtracted from the IGRF model, proton flux, and relativistic and nonrelativistic electron flux during at ~02:00 to 11:00 UT for GOES-15 as a function of MLT and UT on 2 March 2013. The black and gray dashed lines highlight the onset of bright and weak streamers, respectively. GOES-15 was located ~11°W of FSMI ASI and was in the premidnight sector (18:30–23:00 MLT) during the appearance of streamers. Multiple dipolarization-like events (increase in Bz) and high-frequency fluctuations were observed during ~03:50 to 09:00 UT. The first dipolarization activity began at ~03:59 UT when Bz increased abruptly, showing the first sharp peak at ~04:02 UT. After this peak, Bz continued to increase relatively gradually until ~04:35 UT. Interestingly, the first sharp peak in Bz at ~04:02 UT coincided with the near simultaneous increase in both electron and proton flux at all energies. The proton flux did not show any considerable enhancement after this activity. The increase in Bz at ~04:05 to 04:35 UT was associated with the gradual increase in the electron flux at 150 keV–2 MeV (by a factor of ~2.5). The lower energies 40–75 keV did not show considerable enhancement at this time. This dipolarization activity is coincided with the four streamer activities. Note that the substorm onset occurred at ~03:54 UT and the streamer activity started from ~03:57 UT, that is, ~2 to 5 min before the dipolarization. For the second dipolarization-like event at 05:23 UT, the electron flux showed a slight enhancement (by a factor of ~2) at 05:23–06:00 UT, coinciding with the onset of three streamer activities. The streamers at 06:15–07:00 UT were not associated with any considerable variation in Bz and electron flux. The streamers at 08:00 UT occurred ~7 min before the third dipolarization activity at GOES-15. For the third dipolarization activity, the electron flux at higher energies 150 keV–2 MeV showed an enhancement by a factor of ~4 to 6, whereas lower energies (40–75 keV) increased by more than an order of magnitude at ~08:07 to 08:13 UT. While the electron flux at higher energies (150 keV–2 MeV) continued to achieve higher values, the electron flux at lower energies (40–75 keV) showed a second enhancement (by a factor of ~3 to 10) at ~08:20 to 08:30 UT. The increase in the electron flux was rather abrupt and large as compared to the previous two dipolarization activities. Interestingly, the bright and equatorward extending streamers at ~08:19 to 08:30 correspond to the peak in electron flux.

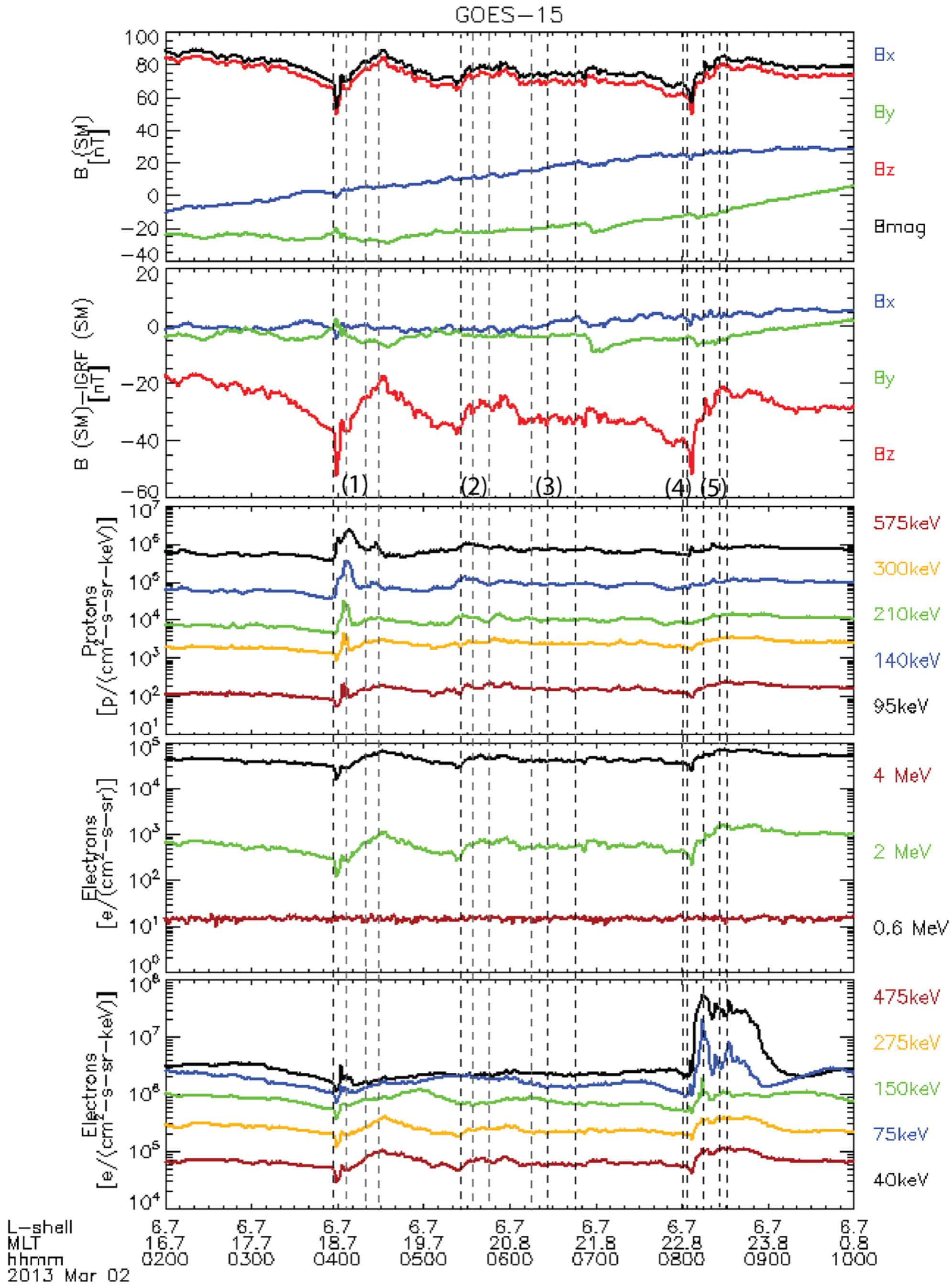

Figure 12. Geostationary Operational Environmental Satellite-15 (GOES-15) observed magnetic field, magnetic field subtracted from the IGRF model, proton flux, and relativistic and nonrelativistic electron flux during ∼02:00 to 10:00 UT as a function of MLT and UT on 2 March 2013. The dashed lines highlight the onset time of streamers over Fort Smith.

4. Discussion and Summary

While the relationship between auroral streamers and magnetic perturbations at auroral latitudes is well-established, here we present a detailed investigation on the association of equatorward extending streamers with magnetic perturbations at the equatorward side of the auroral oval, that is, at subauroral latitudes—an aspect not yet addressed. We made a systematic investigation on the association of equatorward extending streamers, observed during both substorm expansion phase and nonsubstorm times, with negative bay onset and transition bays at auroral and subauroral latitudes, and positive bay and Pi2 pulsation onset at mid and low latitudes. We also investigated the association of auroral streamers with dipolarization and particle flux behavior at geosynchronous orbit. Furthermore, in this study by using high-resolution THEMIS ASI, we could identify isolated bright equatorward extended streamers. Taking advantage of this fact, we examined the evolution characteristics of auroral streamers.

4.1. Association of Auroral Streamers With Ground Magnetic Field Perturbations

Results show that there can be multiple periods of auroral streamers that might not always be associated with a classical substorm auroral onset. The periods of streamers can cause ground magnetometers to respond as expected for a substorm onset. During both geomagnetic substorm and nonsubstorm times, the effect of auroral streamers can extend well equatorward of the auroral oval that existed before the onset of the streamers. Each streamer activity, in general, was accompanied by an abrupt negative deflection in the H-component at auroral and previously subauroral latitudes. In addition, subauroral stations remaining equatorward of the boundary of auroral oval (subauroral latitudes) also show the effect of auroral streamers in terms of negative perturbations but with a magnitude much smaller than those observed within the oval. The stations close to the poleward boundary of the auroral oval showed modest H-component perturbations in response to the auroral onset and PBIs, but the abrupt and large responses were associated with the onset of streamers, consistent with Lyons et al. (2013). The distinct features observed at nominal subauroral latitudes are as follows: (a) the H-component showed positive variations during the PBIs and substorm onset, (b) the start of negative deflection began after the onset of streamers, and (c) the peak negative H-bay coincided with the bright equatorward extending streamers. The ground magnetic decreases at subauroral latitudes were not seen prior to the streamer formation for all four events analyzed here. In conclusion, we identified 18 equatorward extending streamer events (isolated or group of streamers). All these streamer events were associated with a negative H-bay at previously subauroral latitudes as the streamer events lead to an equatorward movement of the auroral oval to those latitudes. For all the events, Pi2 pulsations were observed from auroral to low latitudes.

It is interesting that we have found that the transition bays (Henderson et al., 2006; Rostoker, 1966) at subauroral latitudes (deflection from positive to negative values) can be associated with equatorward extending streamers. The subauroral latitudes in the premidnight sector being under the influence of eastward electrojet display positive magnetic perturbations before the onset of streamers. The FAC by the surge can be another contributor for positive perturbations. As the flow burst in the ionosphere reaches near the equatorward boundary of the auro-ral oval (observed in term of equatorward extending streamers), magnetometers at initially subauroral latitudes become within the auroral oval and show negative magnetic perturbations due to enhanced westward currents. The westward currents that create negative bays at the subauroral latitudes are not likely located at the magnetometer latitudes, but the currents near the oval equatorward boundary create weak negative bays with the considerable negative (upward) Z component.

It can be argued that the boundary of the auroral oval expands equatorward with increasing geomagnetic activity and could reach the latitudes of the nominal subauroral latitudes. In that case, the nominal subauroral latitudes become a part of the auroral oval and should no longer be referred to as subauroral latitudes. Interestingly, the results in this study reveal that it is the equatorward propagating auroral streamer that pushes the boundary of auroral oval toward the lower latitudes. As the streamers extended to lower latitudes, the auroral oval expanded equatorward to reach previously subauroral latitudes. That is the reason why the nominal subauroral latitudes acquired positive deflection before the onset of auroral streamers but showed negative deflection immediately after the onset of streamers with peak negative bay coincided with the well-equatorward extended auroral streamers. It is also interesting to note that after the cessation of auroral streamers, the H-component abruptly deflected toward positive values.

In Event 4, the continuous period of streamers for an extended time (∼5 hr) were associated with the grad-ual decrease in the H-component, apparent at auroral and subauroral latitudes, and in the AL index. In such long-duration cases, the large-scale current system associated with the auroral electrojet might contribute to the overall change in the magnetic field. The continuous presence of localized currents (wedgelets) associated with streamer activities fed the westward electrojet, giving rise to the formation of long-lasting AL. However, the noteworthy feature is the abrupt decreases in the magnetic field associated with the auroral streamers, decreases embedded in the large-scale magnetic field change. For a supersubstorm event (AL = −2,700 nT), Nishimura, Lyons, Gabrielse, Sivadas, et al. (2020) showed that the expansion phase of the supersubstorm is composed of a series of auroral electrojet enhancements on the poleward expanding auroral arc activity, and one of them was associated with an extremely large PBI and streamer. They also argued that the supersubstorm electrojet is fed by a SCW associated with the PBI/streamer, and it was much more localized than the entire extent of the nightside auroral activity. In the present study, we found that irrespective of the association of streamers with substorms, the events of abrupt H-component perturbations are associated with equatorward extending auroral streamers.

It is interesting that the effect of localized streamers reflected in the peak AL values, indicating that AL index may not always be a reliable indicator of the intensity of the substorm onset processes, as also suggested by Lyons et al. (2013). The perturbations in the AL index due to nonsubstorm streamers can be comparable to a real auroral substorm. These results indicate that the ground magnetic perturbations which are typically viewed as signatures of substorm might be associated with auroral streamers. Those events may be regarded as magnetic substorms, but they are not auroral substorms. An interesting additional result of our analysis is that the onset of auroral streamers showed a connection with the ASY-H index, which signifies an intensification of asymmetric ring current in the dusk sector (Nishida, 1978). The bay-like variations of H- and D-components are related to the onset of substorm expansion (Rostoker et al., 1980). Results show that while the SYM-H (symmetric part of the ring current) index remained relatively constant, the ASY-H (the asymmetric part of ring current) index was variable and, in general, acquired higher values during and before the onset of streamers. Liu, Angelopoulos, Zhou, et al. (2013) found a pair of FACs with the R2 sense in the dipolarization front/dipolar flux bundle ahead of the R1 FAC. Previous studies pointed out that the asymmetry in the ring current can be controlled by the balance between R1 and R2 currents (Crooker & Siscoe, 1981; Harel et al., 1981; Iyemori, 1990). The association of bright equatorward extending streamers with the asymmetry in the ring current further supports the conclusion that the ground magnetic perturbations that are usually perceived as the signatures of substorm can be related to the bright auroral streamers.

Traditionally, MPB and Pi2 pulsations have been linked with the formation of the SCW (Baumjohann & Glaβmeier, 1984; Lester et al., 1983), and the buildup of the SCW has been visualized as a fundamental facet of the substorm onset process. A relation between substorms and Pi2 pulsations has been known for a long time (Saito et al., 1976; Yumoto et al., 1989) and linked to the time of expansion onset (Olson, 1999; Pytte et al., 1976). In the absence of substorms, the onset of Pi2 pulsations has been shown to be linked with PBIs (e.g., Kim et al., 2005; Sutcliffe & Lyons, 2002). For substorm events, Nishimura et al. (2012) reported a noteworthy correlation between Pi2 pulsations and quasiperiodic auroral intensifications followed by streamers. Our results indicate that MPB and sudden Pi2 enhancements at mid and low latitude may not be invariably linked with the onset of substorm but may also be related to the onset of PBI and equatorward extending auroral streamers, consistent with earlier studies. The onset of high amplitude Pi2 pulsations at low and mid latitudes coincided with the PBI. We found that every event of PBI was associated with the sudden amplification of Pi2 pulsations at low and mid latitudes which damped later, causing an appearance of jump in the Pi2 amplitude between two PBIs. Whereas, at auroral and subauroral latitudes, the onset of high amplitude Pi2 pulsations showed correspondence with the onset of auroral streamers. The interesting feature of our study is that the amplitude of Pi2 pulsations, particularly at subauroral latitudes, enhanced significantly during the events of bright, equatorward extending streamers. The magnitude of positive bay at mid and low latitudes also enhanced during the events of bright, equatorward extending streamers. As auroral streamers are ionospheric manifestation of BBFs, a remarkable correlation between auroral streamers and Pi2 pulsations support the BBF driven Pi2 model, which proposed that Pi2 pulsations can be generated by compressional pulses produced by high-speed earthward flows in the near-tail (Kepko & Kivelson, 1999; Liu et al., 2017; Shiokawa et al., 1997). The low and mid latitude Pi2 pulsations, which showed correspondence with MPB and PBIs, might also be caused by the FACs of the current wedge, as suggested by Nishimura et al. (2012). The enhancement of MPB during nonsubstorm-time, equatorward-extending streamers suggests that phenomena associated with streamers may contribute to the formation of SCW in an analogous manner as they do during substorm expansion-phase processes.

4.2. Association of Streamers With Dipolarization and Electron Flux Enhancement at Geosynchronous Orbit

The magnetic field dipolarizations associated with a BBF occasionally occur inside geosynchronous orbit (Sergeev et al., 2012) and dipolarizations are often accompanied by injections of energetic particles (e.g., Liu et al., 2016; Reeves et al., 1990; Turner et al., 2017). To examine whether isolated and group of streamers observed in the present study were associated with dipolarization and injections at geosynchronous orbit, we analyzed GOES satellite data. We found that, in general, all auroral streamers were associated with dipolarization and enhancement in electron flux at geosynchronous orbit. Based on one event, Henderson et al. (1998) first reported the injection to be 6.6 RE in association with an auroral streamer during the expansion phase of a substorm. Later, Sergeev et al. (1999) recognized several energetic particle bursts in the electron channels of LANL satellite near midnight, each burst being associated with auroral streamer identified in Polar UV image data. In their study, the burst was defined if the flux increased by at least a factor of 2 in 1 min. Using geotail observations Nakamura, Baumjohann, Brittnacher, et al. (2001) concluded that the earthward flow bursts related to pseudobreakups and small expansions are observed mainly in the region earthward of 15 RE and flows related to high-latitude auro-ral activations and auroral streamers are observed tailward of 15 RE. Recently, for an extremely large PBI and subsequent auroral streamer observed during the extreme substorm event, Nishimura, Lyons, Gabrielse, Sivadas, et al. (2020) showed a two-step dipolarization in the THEMIS and GOES with the second step corresponding to the large PBI/streamer. In the current study we have investigated the dipolarization and injection signature for isolated and streamer groups observed during substorm expansion and nonsubstorm times similar to the conditions of the Henderson et al. (1998) and Nakamura, Baumjohann, Brittnacher, et al. (2001) events. The three distinct features of our observations are as follows: (a) multiple streamers were often associated with multiple events of dipolarization and enhancement in electron flux at geosynchronous orbit, (b) successive group of streamers, in general, emerged during the continuous strengthening of dipolarization and enhancement in electron flux, and (c) bright equatorward extended streamer occurred around the peak enhancement in the electron flux at geosynchronous orbit. Note that one of the limitations of the present study is the fact that, except for the one event (Event 1 at FSIM), the ionospheric footprint of GOES was not located over the FOV of the ASI where streamers were observed. In two cases (at FSMI), the ionospheric footprint of GOES was located 11°W of the ASI FOV, whereas for one event (at FYKN), GOES was located 30°E of the ASI FOV.

4.3. Evolution of Auroral Streamers

In general, all auroral streamers, both isolated and group of streamers, emerged from the poleward boundary of the auroral oval or poleward boundary of the substorm auroral bulge. After onset they extended equatorward and exhibited overall westward motion. This is the general behavior of auroral streamers as reported in previous studies (e.g., Henderson, 2012; Henderson et al., 1994, 1998; Montbriand, 1971; Nishimura et al., 2010; Sergeev et al., 1999). In the present study, we also examined the evolutionary characteristics of streamers. We found that the streamers associated with streamer group emerged continuously and repetitively from the PBI or poleward boundary of the substorm auroral bulge. The growth time of fully grown equatorward extended streamers varied from ∼1 to 2.5 min. Some streamers, mostly associated with repetitive streamers group, were found to be transient in nature (<30 s of lifetime) and did not reach near the equatorward boundary (half-grown streamers). Streamers, in general, showed considerable structuring in terms of detachment from the poleward boundary, folds and curls, eastward tilt, and splitting (Hallinan & Davis, 1970; Pritchett et al., 2014). The lifetime of isolated and streamer groups varied from ∼2 to 6 min. For one case, the lifetime of a bright streamer group was ∼9 min. We estimated the speed of streamers by using eleven well-identified equatorward extended streamers. The streamer events used to estimate the speed is shown in Figures S6–S16 in Supporting Information S1. The speed of streamers varied from 1.8 to 5.2 km/s with an average speed of 3.2 km/s. This speed is larger than the typical speed of ionospheric flow channels, which is ∼400 to 500 m/s estimated by using SuperDARN radars (Gallardo-Lacourt et al., 2014). Gallardo-Lacourt et al. (2014) argued that short-range radar echoes are generally E region backscat-ters. As E-region is dominated by collision, the Doppler speed magnitude is not the full electric field drift, and the magnitude of their Doppler speeds may be underestimated and limited below the ion acoustic speed (∼400 m/s) (Haldoupis, 1989; Koustov et al., 2005). While explaining isolated high-speed auroral streamers, Liu et al. (2008) proposed that Alfvenic fronts at the leading edge of BBFs could be responsible for the high equatorward speeds of auroral streamers. Sergeev et al. (1999) considered a streamer lifetime of ∼2 to 5 min as a lower estimate for the lifetime of individual BBF. They suggested that the 400 km/s threshold velocity of BBF gives a lower estimate of BBF traveling distance about 10–20 RE. Note that our observations are based on only a limited number of events, and therefore, a statistical investigation is required to fully understand the streamer evolution characteristics.

An interesting feature common in all four streamer events is the emergence of a NS aligned bright striation from the lower latitudes that propagates in the poleward direction, reverse motion in comparison to the equatorward propagating streamers. The streamers that follow this convergent motion, equatorward from poleward boundary of the auroral oval and poleward from lower latitudes, were very bright and equatorward extended. The only observation of NS aligned striation emerging from lower latitudes of which we are aware was reported by Liu et al. (2008). Based on one event, they showed that this striation propagated poleward and combined with a high latitude streamer. However, our observations showed that the NS aligned striation emerging from lower latitudes meets with the streamer that extends out from the PBI only in one event (Event 1). In two cases (Events 2 and 3), the striation emerging from lower latitudes propagated poleward and disappeared. In one event (Event 4), both poleward and equatorward motion is observed along the diffuse preexisting streamer that extended out from the PBI. In addition, poleward directed striations were occasional in comparison to equatorward extending streamers. Understanding when and why the poleward directed striations emerged, why bright equatorward extended streamers formed after this equatorward and poleward motion, and how they are associated with the magnetospheric activity warrants further investigation using conjugate space ground measurements.

Acknowledgments

The authors acknowledge use of the SuperMAG ground magnetometer station data (Gjerloev, 2012) and SuperMAG SML and SMU data (Newell & Gjerloev, 2011), available from supermag.jhuapl.edu. The authors acknowledge: (a) NASA contract NAS5-02099 and V. Angelopoulos for use of data from the THEMIS Mission; (b) S. Mende and E. Donovan for use of the ASI data, the CSA for logistical support in fielding and data retrieval from the GBO stations, and NSF for support of GIMNAST through grant AGS-1004736; (c) S. Mende and C. T. Russell for use of the UCLA GMAG data (Russell et al., 2008) and NSF for support through grant AGS-1004814; (d) I. R. Mann, D. K. Milling, and the rest of the CARISMA team for use of CARISMA GMAG data (Mann et al., 2008). CARISMA is operated by the University of Alberta, funded by the Canadian Space Agency; (e) Martin Connors and C. T. Russell and the rest of the AUTUMN/AUTUMNX team for use of the GMAG data; (f) US Geological Survey magnetometers (USGS), original data provided by the USGS Geomagnetism Program (http://geomag.usgs.gov); (g) The Canadian Magnetic Observatory Network (CANMON), maintained and operated by the Geological Survey of Canada, provided the data used in this study (http://www.geomag.nrcan.gc.ca); (h) Alaska magnetometers data were provided by the Geophysical Institute Magnetometer Array operated by the Geophysical Institute, University of Alaska (https://www.gi.alaska.edu/monitors/magnetometer); and (i) Dr. Kanji Hayashi, University of Tokyo for the use of GMAG data. The authors acknowledge the pioneering work by the University of Tokyo (UT), Department of Earth and Planetary Science for the establishment of the STEP (Solar-Terrestrial Energy Program) Polar Network, as well as the long term efforts by UT professor emeritus, Dr. Kanji Hayashi, for continuing to operate and maintain the STEP magnetometer chain for many years. The authors are grateful for this unique, multidecade spanning magnetic data set. Work at the UCLA has been supported by the NSF Grant 2055192 and the NASA Grant 80NSSC20K1314, 80NSSC20K1316, 80NSSC22K0749, 80NSSC22K0751, and AFOSR FA9559-16-1-0364. Work at the Boston University was supported by the NASA Grant 80NSSC18K0657, 80NSSC20K0604, 80NSSC20K0725, 80NSSC21K1321, 80NSSC22K0323, and 80NSSC19K0546, NSF grant AGS-1907698 and AGS-2100975, and AFOSR grant FA9559-16-1-0364. Work at the University of Alabama in Huntsville was supported by the NSF AGS-2120503 and AGS-1952926.

Data Availability Statement

- THEMIS data can be obtained online at themis.ssl.berkeley.edu.
- GOES data are archived at NOAA's National Centers for Environmental Information (NCEI) http://satdat.ngdc.noaa.gov/sem/goes/data/full/.
- The solar wind parameters (IMF Bz) and geomagnetic indices (SYM-H/ASY-H) were obtained from the SPDF, NASA, USA (http://omniweb.gsfc.nasa.gov).

References

Akasofu, S.-I., & Aspnes, J. D. (1982). Auroral effects on power transmission line systems. *Nature*, *295*(5845), 136–137. https://doi.org/10.1038/295136a0

Angelopoulos, V. (2008). The THEMIS mission. *Space Science Reviews*, *141*(1–4), 5–34. https://doi.org/10.1007/s11214-008-9336-1

Angelopoulos, V., Baumjohann, W., Kennel, C., Coroniti, F., Kivelson, M., Pellat, R., et al. (1992). Bursty bulk flows in the inner central plasma sheet. *Journal of Geophysical Research*, *97*(A4), 4027–4039. https://doi.org/10.1029/91JA02701

Angelopoulos, V., Cruce, P., Drozdov, A., Grimes, E. W., Hatzigeorgiu, N., King, D. A., et al. (2019). The Space Physics Environment Data Analysis System (SPEDAS). *Space Science Reviews*, *215*(1), 9. https://doi.org/10.1007/s11214-018-0576-4

Angelopoulos, V., Kennel, C. F., Coroniti, F. V., Pellat, R., Kivelson, M. G., Walker, R. J., et al. (1994). Statistical characteristics of bursty bulk flow events. *Journal of Geophysical Research*, *99*(A11), 21257–21280. https://doi.org/10.1029/94JA01263

Baumjohann, W., & Glaßmeier, K.-H. (1984). The transient response mechanism and Pi2 pulsations at substorm onset—Review and outlook. *Planetary and Space Science*, *32*(11), 1361–1370. https://doi.org/10.1016/0032-0633(84)90079-5

Baumjohann, W., Paschmann, G., & Luhr, H. (1990). Characteristics of high-speed ion flows in the plasma sheet. *Journal of Geophysical Research*, *95*(A4), 3801–3809. https://doi.org/10.1029/JA095iA04p03801

Birn, J., Hesse, M., Haerendel, G., Baumjohann, W., & Shiokawa, K. (1999). Flow braking and the substorm current wedge. *Journal of Geophysical Research*, *104*(A9), 19895–19903. https://doi.org/10.1029/1999JA900173

Boteler, D. H., Pirjola, R. J., & Nevanlinna, H. (1998). The effects of geomagnetic disturbances on electrical systems at the Earth's surface. *Advances in Space Research*, *22*(1), 17–27. https://doi.org/10.1016/S0273-1177(97)01096-X

Campbell, W. H. (1980). Observation of electric currents in the Alaska oil pipeline resulting from auroral electrojet current sources. *Geophysical Journal International*, *61*(2), 437–449. https://doi.org/10.1111/j.1365-246X.1980.tb04325.x

Crooker, N. U., & Siscoe, G. L. (1981). Birkeland currents as the cause of the low-latitude asymmetric disturbance field. *Journal of Geophysical Research*, *86*(A13), 11201–11210. https://doi.org/10.1029/JA086iA13p11201

De la Beaujardière, O., Lyons, L. R., Ruohoniemi, J. M., Friis-Christensen, E., Danielsen, C., Rich, F. J., & Newell, P. T. (1994). Quiet-time intensifications along the poleward auroral boundary near midnight. *Journal of Geophysical Research*, *99*(A1), 287–298. https://doi.org/10.1029/93JA01947

Engebretson, M. J., Steinmetz, E. S., Posch, J. L., Pilipenko, V. A., Moldwin, M. B., Connors, M. G., et al. (2019). Nighttime magnetic perturbation events observed in Arctic Canada: 2. Multiple-instrument observations. *Journal of Geophysical Research: Space Physics*, *124*(9), 7459–7476. https://doi.org/10.1029/2019JA026797

Forsyth, C., Fazakerley, A. N., Rae, I. J., Watt, J. C. E., Murphy, K., Wild, J. A., et al. (2014). In situ spatiotemporal measurements of the detailed azimuthal substructure of the substorm current wedge. *Journal of Geophysical Research: Space Physics*, *119*(2), 927–946. https://doi.org/10.1002/2013ja019302

Forsyth, C., Sergeev, V. A., Henderson, M. G., Nishimura, Y., & Gallardo-Lacourt, B. (2020). Physical processes of meso-scale, dynamic auroral forms. *Space Science Reviews*, *216*(4), 46. https://doi.org/10.1007/s11214-020-00665-y

Gabrielse, C., Nishimura, Y., Lyons, L., Gallardo-Lacourt, B., Deng, Y., & Donovan, E. (2018). Statistical properties of mesoscale plasma flows in the nightside high-latitude ionosphere. *Journal of Geophysical Research: Space Physics*, *123*(8), 6798–6820. https://doi.org/10.1029/2018JA025440

Gallardo-Lacourt, B., Nishimura, Y., Lyons, L. R., Zou, S., Angelopoulos, V., Donovan, E., et al. (2014). Coordinated SuperDARN THEMIS ASI observations of mesoscale flow bursts associated with auroral streamers. *Journal of Geophysical Research: Space Physics*, *119*(1), 142–150. https://doi.org/10.1002/2013JA019245

Gjerloev, J. W. (2012). The SuperMAG data processing technique. *Journal of Geophysical Research*, *117*(A9), A09213. https://doi.org/10.1029/2012JA017683

Haldoupis, C. (1989). A review on radio studies of auroral E region ionospheric irregularities. *Annales Geophysicae*, *7*(1), 239–243. https://doi.org/10.1007/s00585-994-0040-5

Hallinan, T. J., & Davis, T. N. (1970). Small-scale auroral arc distortions. *Planetary and Space Science*, *18*(12), 1735–1744. https://doi.org/10.1016/0032-0633(70)90007-3

Harel, M., Wolf, R. A., Spiro, R. W., Reiff, P. H., Chen, C.-K., Burke, W. J., et al. (1981). Quantitative simulation of a magnetospheric substorm 2. Comparison with observations. *Journal of Geophysical Research*, *86*(A4), 2242–2260. https://doi.org/10.1029/JA086iA04p02242

Henderson, M. G. (2012). Auroral substorms, poleward boundary activations, auroral streamers, omega bands, and onset precursor activity, Auroral phenomenology and magnetospheric processes. In A. Keiling, E. Donovan, F. Bagenal, & T. Karlsson (Eds.), *Earth and other planets, Geophysical Monograph Series* (Vol. 197, pp. 39–54). American Geophysical Union.

Henderson, M. G., Reeves, G. D., & Murphree, J. S. (1994). The activation of the dusk-side and the formation of north-south aligned structures during substorms. In J. R. Kan, J. D. Craven, & S.-I. Akasofu (Eds.), *Proceedings Second International Conference on Substorms (ICS-2)* (pp. 37). Geophysical Institute, University of Alaska Fairbanks.

Henderson, M. G., Reeves, G. D., & Murphree, J. S. (1998). Are north–south aligned auroral structures an ionospheric manifestation of bursty bulk flows? *Geophysical Research Letters*, *25*(19), 3737–3740. https://doi.org/10.1029/98GL02692

Henderson, M. G., Skoug, R., Donovan, E., Thomsen, M. F., Reeves, G. D., Denton, M. H., et al. (2006). Substorms during the 10–11 August 2000 sawtooth event. *Journal of Geophysical Research*, *111*(A6), A06206. https://doi.org/10.1029/2005JA011366

Iijima, T., & Nagata, T. (1972). Signatures for substorm development of the growth phase and expansion phase. *Planetary and Space Science*, *20*(7), 1095–1112. https://doi.org/10.1016/0032-0633(72)90219-X

Iijima, T., & Potemra, T. A. (1978). Large-scale characteristics of field-aligned currents associated with substorms. *Journal of Geophysical Research*, *83*(A2), 599. https://doi.org/10.1029/JA083iA02p00599

Iyemori, T. (1990). Storm-time magnetospheric currents inferred from mid-latitude geomagnetic field variations. *Journal of Geomagnetism and Geoelectricity*, *42*(11), 1249–1265. https://doi.org/10.5636/jgg.42.1249

Kauristie, K., Sergeev, V. A., Amm, O., Kubyshkina, M. V., Jussila, J., Donovan, E., & Liou, K. (2003). Bursty bulk flow intrusion to the inner plasma sheet as inferred from auroral observations. *Journal of Geophysical Research*, *108*(A1), 1040. https://doi.org/10.1029/2002JA009371

Kauristie, K., Sergeev, V. A., Kubyshkina, M., Pulkkinen, T. I., Angelopoulos, V., Phan, T., et al. (2000). Ionospheric current signatures of transient plasma sheet flows. *Journal of Geophysical Research*, *105*(A5), 10677–10690. https://doi.org/10.1029/1999ja900487

Kepko, L., & Kivelson, M. (1999). Generation of Pi2 pulsations by bursty bulk flows. *Journal of Geophysical Research*, *104*(A11), 25021–25034. https://doi.org/10.1029/1999JA900361

Kim, K.-H., Takahashi, K., Lee, D.-H., Sutcliffe, P. R., & Yumoto, K. (2005). Pi2 pulsations associated with poleward boundary intensifications during the absence of substorms. *Journal of Geophysical Research*, *110*(A1), A01217. https://doi.org/10.1029/2004JA010780

Koustov, A. V., Danskin, D. W., Makarevitch, R. A., & Gorin, J. D. (2005). On the relationship between the velocity of E region HF echoes and E x B plasma drift. *Annales Geophysicae*, *23*(2), 371–378. https://doi.org/10.5194/angeo-23-371-2005

Kozyreva, O. V., Pilipenko, V. A., Belakhovsky, V. B., & Sakharov, Y. A. (2018). Ground geomagnetic field and GIC response to March 17, 2015, storm. *Earth Planets and Space*, *70*(1), 157. https://doi.org/10.1186/s40623-018-0933-2

Lester, M., Hughes, J. W., & Singer, H. J. (1983). Polarization patterns of Pi2 magnetic pulsations and the substorm current wedge. *Journal of Geophysical Research*, *88*(A10), 7958–7966. https://doi.org/10.1029/JA088iA10p07958

Liu, J., Angelopoulos, V., Chu, X., Zhou, X., & Yue, C. (2015). Substorm current wedge composition by wedgelets. *Geophysical Research Letters*, *42*(6), 1669–1676. https://doi.org/10.1002/2015gl063289

Liu, J., Angelopoulos, V., Runov, A., & Zhou, X.-Z. (2013). On the current sheets surrounding dipolarizing flux bundles in the magnetotail: The case for wedgelets. *Journal of Geophysical Research: Space Physics*, *118*(5), 2000–2020. https://doi.org/10.1002/jgra.50092

Liu, J., Angelopoulos, V., Zhang, X. J., Turner, D. L., Gabrielse, C., Runov, A., et al. (2016). Dipolarizing flux bundles in the CIS-geosynchronous magnetosphere: Relationship between electric fields and energetic particle injections. *Journal of Geophysical Research: Space Physics*, *121*(2), 1362–1376. https://doi.org/10.1002/2015JA021691

Liu, J., Angelopoulos, V., Zhang, X.-J., Runov, A., Artemyev, A., Plaschke, F., et al. (2017). Ultralow frequency waves deep inside the inner magnetosphere driven by dipolarizing flux bundles. *Journal of Geophysical Research: Space Physics*, *122*(10), 10112–10128. https://doi.org/10.1002/2017JA024270

Liu, J., Angelopoulos, V., Zhou, X.-Z., & Runov, A. (2014). Magnetic flux transport by dipolarizing flux bundles. *Journal of Geophysical Research: Space Physics*, *119*(2), 909–926. https://doi.org/10.1002/2013JA019395

Liu, J., Angelopoulos, V., Zhou, X.-Z., Runov, A., & Yao, Z. H. (2013). On the role of pressure and flow perturbations around dipolarizing flux bundles. *Journal of Geophysical Research: Space Physics*, *118*(11), 7104–7118. https://doi.org/10.1002/2013JA019256

Liu, W. W., Liang, J., Donovan, E. F., Trondsen, T., Baker, G., Sofko, G., et al. (2008). Observation of isolated high-speed auroral streamers and their interpretation as optical signatures of Alfvén waves generated by bursty bulk flows. *Geophysical Research Letters*, *35*(4), L04104. https://doi.org/10.1029/2007GL032722

Lyons, L. R., Gallardo-Lacourt, B., Zou, S., Weygand, J. M., Nishimura, Y., Li, W., et al. (2016). The 17 March 2013 storm: Synergy of observations related to electric field modes and their ionospheric and magnetospheric effects. *Journal of Geophysical Research: Space Physics*, *121*(11), 10880–10897. https://doi.org/10.1002/2016JA023237

Lyons, L. R., Nagai, T., Blanchard, G. T., Samson, J. C., Yamamoto, T., Mukai, T., et al. (1999). Association between Geotail plasma flows and auroral poleward boundary intensifications observed by CANOPUS photometers. *Journal of Geophysical Research*, *104*(A3), 4485–4500. https://doi.org/10.1029/1998JA900140

Lyons, L. R., Nishimura, Y., Donovan, E., & Angelopoulos, V. (2013). Distinction between auroral substorm onset and traditional ground magnetic onset signatures. *Journal of Geophysical Research: Space Physics*, *118*(7), 4080–4092. https://doi.org/10.1002/jgra.50384

Lyons, L. R., Nishimura, Y., Xing, X., Runov, A., Angelopoulos, V., Donovan, E., & Kikuchi, T. (2012). Coupling of dipolarization front flow bursts to substorm expansion phase phenomena within the magnetosphere and ionosphere. *Journal of Geophysical Research*, *117*(A2), A02212. https://doi.org/10.1029/2011ja017265

Mann, I. R., Milling, D. K., Rae, I. J., Ozeke, L. G., Kale, A., Kale, Z. C., et al. (2008). The upgraded CARISMA magnetometer array in the THEMIS era. *Space Science Reviews*, *141*(1–4), 413–451. https://doi.org/10.1007/s11214-008-9457-6

McPherron, R. L. (1972). Substorm related changes in the geomagnetic tail: The growth phase. *Planetary and Space Science*, *20*(9), 1521–1539. https://doi.org/10.1016/0032-0633(72)90054-2

McPherron, R. L., Russell, C. T., & Aubry, M. P. (1973). Satellite studies of magnetospheric substorms on August 15, 1968: 1. State of the magnetosphere. *Journal of Geophysical Research*, *78*(16), 3044–3053. https://doi.org/10.1029/JA078i016p03044

Mende, S. B., Harris, S. E., Frey, H. U., Angelopoulos, V., Russell, C. T., Donovan, E., et al. (2008). The THEMIS array of ground-based observatories for the study of auroral substorms. *Space Science Reviews*, *141*(1–4), 357–387. https://doi.org/10.1007/s11212-008-9380-x

Montbriand, L. E. (1971). The proton aurora substorm. In B. M. McCormac (Ed.), *The radiating atmosphere* (pp. 366–373). D. Reidel.

Nakamura, R., Baumjohann, W., Brittnacher, M., Sergeev, V. A., Kubyshkina, M., Mukai, T., & Liou, K. (2001). Flow bursts and auroral activations: Onset timing and foot point location. *Journal of Geophysical Research*, *106*(A6), 10777–10789. https://doi.org/10.1029/2000ja000249

Nakamura, R., Baumjohann, W., Klecker, B., Bogdanova, Y., Balogh, A., Reme, H., et al. (2002). Motion of the dipolarization front during a flow burst event observed by Cluster. *Geophysical Research Letters*, *29*(20), 1942. https://doi.org/10.1029/2002GL015763

Nakamura, R., Baumjohann, W., Schödel, R., Brittnacher, M., Sergeev, V. A., Kubyshkina, M., et al. (2001). Earthward flow bursts, auroral streamers, and small expansions. *Journal of Geophysical Research*, *106*(A6), 10791–10802. https://doi.org/10.1029/2000JA000306

Nakamura, R., Oguti, T., Yamamoto, T., & Kokubun, S. (1993). Equatorward and poleward expansion of the auroras during auroral substorms. *Journal of Geophysical Research*, *98*(A4), 5743–5759. https://doi.org/10.1029/92JA02230

Newell, P. T., & Gjerloev, J. W. (2011). Evaluation of SuperMAG auroral electrojet indices as indicators of substorms and auroral power. *Journal of Geophysical Research*, *116*(A12), A12211. https://doi.org/10.1029/2011JA016779

Ngwira, C. M., Pulkkinen, A. A., Bernabeu, E., Eichner, J., Viljanen, A., & Crowley, G. (2015). Characteristics of extreme geoelectric fields and their possible causes: Localized peak enhancements. *Geophysical Research Letters*, *42*(17), 6916–6921. https://doi.org/10.1002/2015GL065061

Ngwira, C. M., Pulkkinen, A., Kuznetsova, M. M., & Glocer, A. (2014). Modeling extreme "Carrington-type" space weather events using three-dimensional MHD code simulations. *Journal of Geophysical Research: Space Physics*, *119*(6), 4456–4474. https://doi.org/10.1002/2013JA019661

Ngwira, C. M., Sibeck, D. G., Silveira, M. D. V., Georgiou, M., Weygand, J. M., Nishimura, Y., & Hampton, D. (2018). A study of intense local dB/dt variations during two geomagnetic storms. *Space Weather*, *16*(6), 676–693. https://doi.org/10.1029/2018SW001911

Nishida, A. (1978). *Geomagnetic diagnosis of the magnetosphere*. Springer.

Nishimura, Y., Lyons, L. R., Gabrielse, C., Sivadas, N., Donovan, E. F., Varney, R. H., et al. (2020). Extreme magnetosphere-ionosphere-thermosphere responses to the 5 April 2010 supersubstorm. *Journal of Geophysical Research: Space Physics*, *125*(4), e2019JA027654. https://doi.org/10.1029/2019JA027654R

Nishimura, Y., Lyons, L. R., Gabrielse, C., Weygand, J. M., Donovan, E. F., & Angelopoulos, V. (2020). Relative contributions of large-scale and wedgelet currents in the substorm current wedge. *Earth Planets and Space*, *72*(1), 106. https://doi.org/10.1186/s40623-020-01234-x

Nishimura, Y., Lyons, L. R., Kikuchi, T., Angelopoulos, V., Donovan, E., Mende, S., et al. (2012). Formation of substorm Pi2: A coherent response to auroral streamers and currents. *Journal of Geophysical Research*, *117*(A9), A09218. https://doi.org/10.1029/2012JA017889

Nishimura, Y., Lyons, L., Zou, S., Angelopoulos, V., & Mende, S. (2010). Substorm triggering by new plasma intrusion: THEMIS all-sky imager observations. *Journal of Geophysical Research*, *115*(A7), A07222. https://doi.org/10.1029/2009JA015166

Olson, J. V. (1999). Pi2 pulsations and substorm onsets: A review. *Journal of Geophysical Research*, *104*(A8), 17499–17520. https://doi.org/10.1029/1999ja900086

Palin, L., Jacquey, C., Opgenoorth, H., Connors, M., Sergeev, V., Sauvaud, J.-A., et al. (2015). Three-dimensional current systems and ionospheric effects associated with small dipolarization fronts. *Journal of Geophysical Research: Space Physics*, *120*(5), 3739–3757. https://doi.org/10.1002/2015ja021040

Paschmann, G., Haaland, S., & Treumann, R. (2012). *Auroral plasma physics*. Springer Science & Business Media.

Pirjola, R. (2005). Effects of space weather on high-latitude ground systems. *Advances in Space Research*, *36*(12), 2231–2240. https://doi.org/10.1016/j.asr.2003.04.074

Pritchett, P. L., Coroniti, F. V., & Nishimura, Y. (2014). The kinetic ballooning/interchange instability as a source of dipolarization fronts and auroral streamers. *Journal of Geophysical Research: Space Physics*, *119*(6), 4723–4739. https://doi.org/10.1002/2014JA019890

Pulkkinen, A., Lindahl, S., Viljanen, A., & Pirjola, R. (2005). Geomagnetic storm of 29–31 October 2003: Geomagnetically induced currents and their relation to problems in the Swedish high-voltage power transmission system. *Space Weather*, *3*(8), S08C03. https://doi.org/10.1029/2004SW000123

Pulkkinen, A., Thomson, A., Clarke, E., & McKay, A. (2003). April 2000 geomagnetic storm: Ionospheric drivers of large geomagnetically induced currents. *Annales Geophysicae*, *21*(3), 709–717. https://doi.org/10.5194/angeo-21-709-2003

Pytte, T., McPherron, R. L., & Kokubun, S. (1976). The ground signatures of the expansion phase during multiple onset substorms. *Planetary and Space Science*, *24*(12), 1115–1132. https://doi.org/10.1016/0032-0633(76)90149-5

Reeves, G. D., Fritz, T. A., Cayton, T. E., & Belian, R. D. (1990). Multi-satellite measurements of the substorm injection region. *Geophysical Research Letters*, *17*(11), 2015–2018. https://doi.org/10.1029/GL017i011p02015

Rostoker, G. (1966). Mid-latitude transition bays and their relation to the spatial movement of overhead current systems. *Journal of Geophysical Research*, *71*(1), 79–95. https://doi.org/10.1029/JZ071i001p00079

Rostoker, G. (1968). Macrostructure of geomagnetic bays. *Journal of Geophysical Research*, *73*(13), 4217–4229. https://doi.org/10.1029/JA073i013p04217

Rostoker, G. (1991). Some observational constraints for substorm models. In J. R. Kan, T. A. Potemra, S. Kokubun, & T. Iijima (Eds.), *Magnetospheric Substorms Geophysical Monograph Series* (Vol. 64, pp. 61). AGU.

Rostoker, G., Akasofu, S. I., Foster, J., Greenwald, R., Kamide, Y., Kawasaki, K., et al. (1980). Magnetospheric substorm – Definition and signatures. *Journal of Geophysical Research*, *85*(A4), 1663–1668. https://doi.org/10.1029/ja085ia04p01663

Russell, C. T., Chi, P. J., Dearborn, D. J., Ge, Y. S., Kuo-Tiong, B., Means, J. D., et al. (2008). THEMIS ground-based magnetometers. *Space Science Reviews*, *141*(1–4), 389–412. https://doi.org/10.1007/s11214-008-9337-0

Saito, T. (1969). Geomagnetic pulsations. *Space Science Reviews*, *10*(3), 319. https://doi.org/10.1007/bf00203620

Saito, T., Sakurai, T., & Koyama, Y. (1976). Mechanism of association Pi2 pulsation and magnetospheric substorm. *Journal of Atmospheric and Terrestrial Physics*, *38*(12), 1265–1277. https://doi.org/10.1016/0021-9169(76)90135-5

Sakurai, T., & Saito, T. (1976). Magnetic pulsation Pi2 and substorm onset. *Planetary and Space Science*, *24*(6), 573–575. https://doi.org/10.1016/0032-0633(76)90135-5

Sergeev, V. A. (1974). On the longitudinal localization of the substorm active region and its changes during the substorm. *Planetary and Space Science*, *22*(9), 1341–1343. https://doi.org/10.1016/0032-0633(74)90055-5

Sergeev, V. A., Chernyaev, I. A., Dubyagin, S. V., Miyashita, Y., Angelopoulos, V., Boakes, P. D., et al. (2012). Energetic particle injections to geostationary orbit: Relationship to flow bursts and magnetospheric state. *Journal of Geophysical Research*, *117*(A10), A10207. https://doi.org/10.1029/2012JA017773

Sergeev, V. A., Liou, K., Meng, C.-I., Newell, P., Brittnacher, M., Parks, G., & Reeves, G. (1999). Development of auroral streamers in association with localized impulsive injections to the inner magnetotail. *Geophysical Research Letters*, *26*(3), 417–420. https://doi.org/10.1029/1998GL900311

Sergeev, V. A., Sauvaud, J. A., Popescu, D., Kovrazhkin, R. A., Liou, K., Newell, P. T., et al. (2000). Multiple-spacecraft observation of a narrow transient plasma jet in the Earth's plasma sheet. *Geophysical Research Letters*, *27*(6), 851–854. https://doi.org/10.1029/1999GL010729

Shiokawa, K., Baumjohann, W., & Haerendel, G. (1997). Braking of high–speed flows in the near–Earth tail. *Geophysical Research Letters*, *24*(10), 1179–1182. https://doi.org/10.1029/97GL01062

Singer, H. J., Matheson, L., Grubb, R., Newman, A., & Bouwer, D. (1996). Monitoring space weather with the GOES magnetometers. In E. Washwell (Ed.), *GOES-8 and beyond* (Vol. 2812, pp. 299–308). NOAA Space Environment Center. https://doi.org/10.1117/12.254077

Sutcliffe, P., & Lyons, L. (2002). Association between quiet-time Pi2 pulsations, poleward boundary intensifications, and plasma sheet particle fluxes. *Geophysical Research Letters*, *29*(9), 1293. https://doi.org/10.1029/2001GL014430

Turner, D. L., Fennell, J., Blake, J., Claudepierre, S., Clemmons, J., Jaynes, A., et al. (2017). Multipoint observations of energetic particle injections and substorm activity during a conjunction between Magnetospheric Multiscale (MMS) and Van Allen Probes. *Journal of Geophysical Research: Space Physics*, *122*(11), 11481–11504. https://doi.org/10.1002/2017JA024554

Viljanen, A. (1997). The relation between geomagnetic variations and their time derivatives and implications for estimation of induction risks. *Geophysical Research Letters*, *24*(6), 631–634. https://doi.org/10.1029/97GL00538

Viljanen, A., Tanskanen, E. I., & Pulkkinen, A. (2006). Relation between substorm characteristics and rapid temporal variations of the ground magnetic field. *Annales Geophysicae*, *24*(2), 725–733. https://doi.org/10.5194/angeo-24-725-2006

Wei, D., Dunlop, M. W., Yang, J., Dong, X., Yu, Y., & Wang, T. (2021). Intense dB/dt variations driven by near-Earth bursty bulk flows (BBFs): A case study. *Geophysical Research Letters*, *48*(4), e2020GL091781. https://doi.org/10.1029/2020GL091781

Weygand, J. M., Engebretson, M. J., Pilipenko, V. A., Steinmetz, E. S., Moldwin, M. B., Connors, M. G., et al. (2021). SECS analysis of nighttime magnetic perturbation events observed in Arctic Canada. *Journal of Geophysical Research: Space Physics*, *126*(11), e2021JA029839. https://doi.org/10.1029/2021JA029839

Yumoto, K., Takahashi, K., Saito, T., Menk, F. W., Fraser, B. J., Potemra, T. A., & Zanetti, L. J. (1989). Some aspects of the relation between Pi 1-2 magnetic pulsations observed at L = 1.3–2.1 on the ground and substorm-associated magnetic field variations in the near-Earth magnetotail observed by AMPTE CCE. *Journal of Geophysical Research*, *94*(A4), 3611–3618. https://doi.org/10.1029/JA094iA04p03611

Zesta, E., Lyons, L., & Donovan, E. (2000). The auroral signature of Earthward flow bursts observed in the magnetotail. *Geophysical Research Letters*, *27*(20), 3241–3244. https://doi.org/10.1029/2000gl000027